LMSC/HREC A783082
Revision A

LOCKHEED MISSILES & SPACE COMPANY

HUNTSVILLE RESEARCH & ENGINEERING CENTER

HUNTSVILLE RESEARCH PARK

4800 BRADFORD DRIVE, HUNTSVILLE, ALABAMA

N66-22272

FIRST INTERIM REPORT

PRELIMINARY DESIGN STUDY OF A LUNAR GRAVITY SIMULATOR

29 July 1966

Contract NAS8-20351

Prepared for George C. Marshall Space Flight Center
Huntsville, Alabama

PREPARED BY: R. B. Wysor
Systems Engineering

APPROVED BY: R. S. Paulnock
Mgr., Systems Engineering

R. S. Paulnock
for J. S. Farrior
Resident Manager

FOREWORD

This report was prepared by the Lockheed Missiles & Space Company, Huntsville Research & Engineering Center, to document the accomplishments of the first five weeks of study efforts (ending 22 July 1966) for the Preliminary Design of a Lunar Gravity Simulator, Contract NAS8-20351. The study is being conducted by the Systems Engineering Department at HREC under the direction of Mr. R. S. Paulnock, Manager, and R. B. Wysor, Project Engineer. The study program is sponsored by the Advanced Systems Office of Marshall Space Flight Center under the technical direction of Mr. Herbert Schaefer, Principal COR, and Mr. Robert R. Belew, Alternate COR.

Technical data in this report will be delivered to NASA/MSFC technical personnel at an informal presentation scheduled for 1 August 1966.

CONTENTS

Section 1
INTRODUCTION

The Lunar Gravity Simulator (LGS) is a system planned for the evaluation of full scale Lunar Surface Vehicles (LSV) over simulated Lunar terrain in an Earth's gravity environment. The purpose of such a system will be to:

- Substantiate the LSV mobility system performance and lifetime parameters under simulated loading conditions as may occur from the 1/6 g environment and the anticipated obstacle, slope and velocity combination.
- Establish the confidence level of the ability to design the mobility systems for various LSV configurations.
- Determine the effect of the vehicle dynamic behavior on the vehicle operator and the man-machine relationship in a 1/6 g environment.
- Train astronauts in handling LSV's in a 1/6 g environment.

With these objectives in mind, LMSC has been conducting a Preliminary Design Study of a Lunar Gravity Simulator System under contract to the Marshall Space Flight Center. This study effort will encompass a 15 week period which will be subdivided into three five-week intervals. This report describes the tasks and accomplishments of the first five-week period ending 22 July 1966, and the tasks and approaches planned for subsequent study efforts.

Figure 1 depicts the overall LGS study program plan (Task, Schedule and Manloading). The tasks for the first five-week period were the initial tasks for the preliminary design and analysis of a two-dimensional* Lunar Gravity Simulator. These tasks were:

1.1 Survey of existing information and concepts

* A two-dimensional LGS restricts LSV motion to a vertical plane with freedom in the roll, pitch, vertical and horizontal dimensions.

1.2 Identification of test parameters - establish math model of LGS system and candidate LSV's.

1.3 Analysis and selection of suspension device and drive system concepts.

1.7 Design, layouts and component specifications of 2-D LGS system.

The following discussion describes the accomplishments on these tasks and the work planned on subsequent tasks outlined in Figure 1.

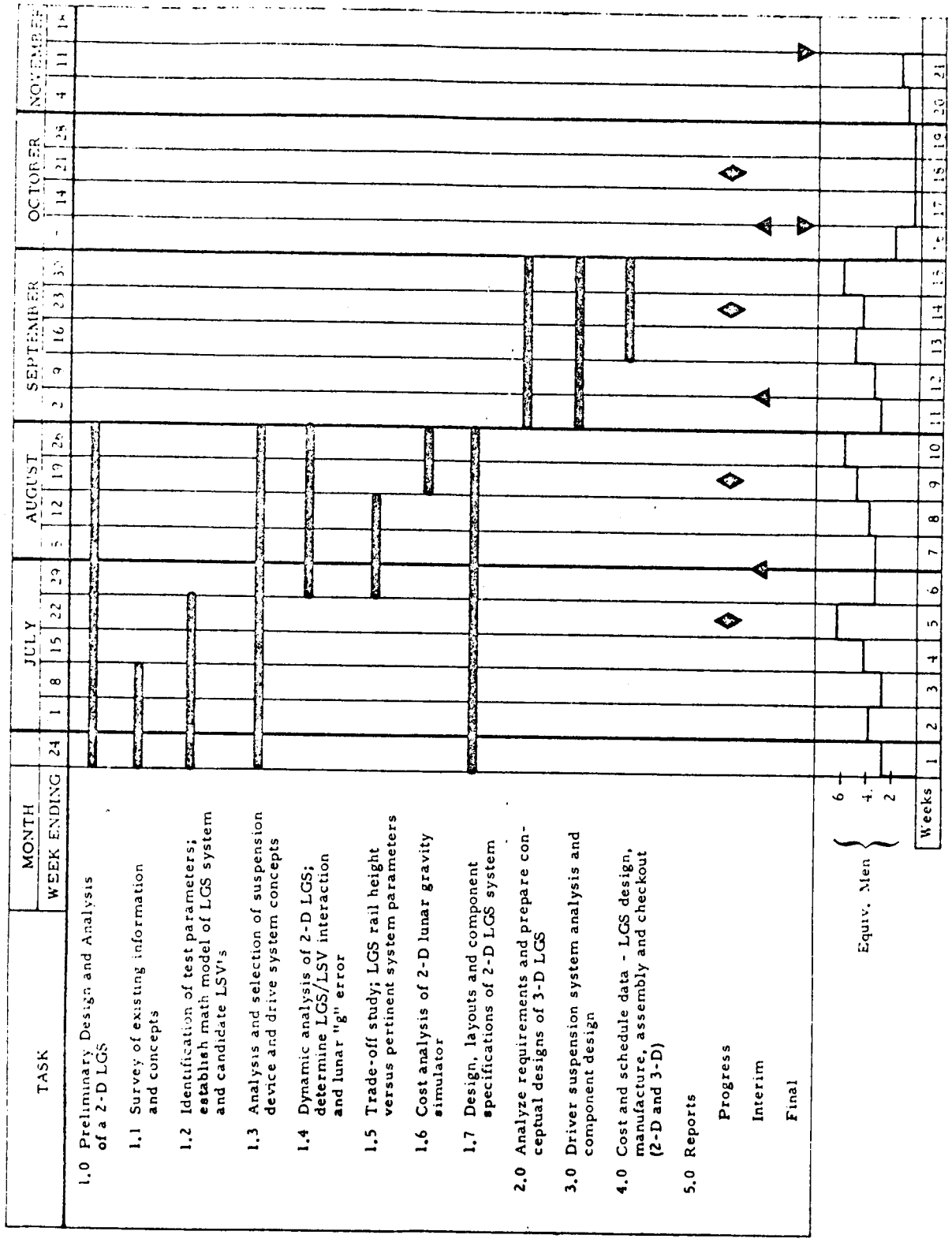

Figure 1 - Program Plan

Section 2
SURVEY OF EXISTING INFORMATION AND CONCEPTS

The objective of this task is to review the current technology of horizontal gravity simulators and related equipment to establish the present state of the art and to offer background information for the preliminary design and analysis efforts to follow. This survey has included a review of 32 documents which were obtained as a result of a literature survey by the Redstone Scientific Information Center and as a result of contact with NASA/MSFC technical personnel. Seven documents were selected as contributing information pertinent to the preliminary design and analysis of the Lunar Gravity Simulator. A summary of the pertinent information in these documents is given in Figure 2. It should be noted that the documents are exclusive of those pertaining to the mobility system characteristics of the candidate Lunar Surface Vehicles which were obtained as a part of Task 1.2 (the identification of test parameters).

The information presented in Figure 2 may be divided into three groups of data: (1) design concepts of a lunar gravity simulator for Marshall Space Flight Center; (2) conceptual design studies for a space motion simulator for the Manned Spacecraft Center; and (3) the techniques and equipment used in conjunction with the Langley Research Center's Lunar Landing Facility. The corresponding documents are grouped according to source and sponsor in Figure 2. The last column in this chart relates the technology useful to the LGS program. Other pertinent aspects are discussed in the following paragraphs.

MARSHALL SPACE FLIGHT CENTER STUDIES

The work by Northrop in report NSLE 30-44, was a program to prepare a conceptual analysis of a variety of lunar gravity simulation devices

Source	Sponsor	Document	Essential Content	Related Technology useful to LGS Program
Northrop Space Laboratories	NASA-MSFC	NSL E 30-44 April 1965	Lunar Gravity Simulator for MTA Test Program	Established ground rules and design criteria; Reviewed facilties for use in program; Compared and chose a horizontal plane concept from several types; Support systems used for sensing position changes.
Northrop Space Laboratories	NASA-MSFC	NSL E 30-61 August 1965	Continued Design Study for a Limited Capability Simulator	Considered additional inclined plane concepts, but found horizontal plane concept best. Continued design, using a limited capability system (no y-axis capability - straight line operation).
Northrop Space Laboratories	NASA-MSFC	NSL E 30-80 March 1966	Feasibility Study of Langley LRF for MTA Tests	Detailed study of rework needed to adopt Langley Lunar Landing Research Facility for MTA Tests. Detailed sequential test program for MTA.
Aircraft Armaments	NASA-MSC	ER-2938 January 1963	Conceptual Design of a Space Motion Simulator	Structural design and analysis; Instrumentation for sensing displacement, velocity, acceleration; Control system for main generator; Translation system selection criteria.
Aircraft Armaments	NASA-MSC	ER-3377 March 1964	Continued Study of a Space Motion Simulator	Inclusion in analysis of viscoelastic damping of main structure; Revision of drive motors recommendation to an ironless motor; Use of silicon controlled rectifiers for control; Detailed study of harness arrangements for astronauts.
Langley Research Center	NASA-Langley	NASA TND-2636 February 1965	Lunar Landing Simulator Tests of Mock-up LEM vehicles	Describes servo hydraulic motor driven winch and cable support system for simulating 1/6 g environment.
Langley Research Center	NASA-Langley	NASA-STAR X63-14590 July 1962	Langley Lunar Landing Research Facility	Describes facility dimensional and performance data.

Figure 2 - Summary of Information Sources for Gravity Simulators

suitable for the Block II Mobility Test Article (MTA) program. The specific objectives were: (1) establish design requirements directly applicable to the MTA test program; (2) survey and analyze existing facilities for suitability; (3) determine several conceptual designs of simulators which satisfy the design requirements; and (4) perform cost estimates and a trade-off analysis of the various conceptual designs. The design concepts were to be capable of testing vehicles weighing to 10,000 pounds and were to take into consideration the various vehicle configurations which were selected, including four-wheel rigid chassis and six-wheel articulated chassis design. The velocities and accelerations required of the lunar gravity simulator as determined by Northrop are based upon the requirements of the test program in this report.

A check of existing facilities revealed that only the Langley Research Center's Lunar Landing Facility (LLRF) approached the required operational characteristics, but it was still inadequate. Because of this, other facilities were surveyed, including MSFC in Report E 30-61. The conclusion was that an outside installation at Building 4755 was a remote possibility mainly due to crane speed. Although there were many deficiencies at the Langley LLRF, a detailed analysis was conducted and is reported in Report E 30-80. The conclusion was that the cost and available scheduled test time precluded the use of the LLRF.

Three horizontal plane and two inclined plane simulator concepts were examined in report E 30-44. A vehicle performance analysis revealed that all of the horizontal plane concepts would simulate the lunar gravity more realistically than either of the inclined plane concepts. The horizontal plane concepts were based on an overhead support system above a "horizontal" test track. A servo system supports 5/6 of the vehicle weight via a single cable to the chassis center of gravity and a constant force device attached from each wheel to a suspension frame just above the vehicle.

The major contributions of these reports were: (1) ground rules; (2) design criteria; (3) review of existing facilities; (4) vehicle support

system; (5) controls system; and (6) translational system. (The Northrop design did not consider dynamic conditions in any detail. Any actual design effort must include these factors in the basic design.)

Report NSL E 30-61 deals mostly with efforts to adapt the inclined plane concepts to minimize the basic horizontal plane's inherent advantages. These were generally unsuccessful. In addition, consideration was given to the design of a limited capability simulator. This concept is the same as in report SL E 30-61, except that it is limited to straight-line operation.

To summarize, these reports show that the concept of a horizontal plane lunar gravity simulator is the best method of testing lunar surface vehicles, that the simulation will give adequate information for further design and that the detail design must be based on a combination of factors; namely, cost, schedule time and degree of simulation desired.

MANNED SPACECRAFT CENTER STUDIES

The design of a space motion simulator at the Manned Spacecraft Center is illustrated in Figure 3. This study, conducted by Aircraft Armaments Incorporated, investigated a device capable of simulating the motion of a man or vehicle in space or in a reduced gravity environment. The device has complete six-degrees-of-freedom. The motion of the device can be programmed from forces generated by the payload, by control signals from the astronaut or external drive signals. Although this system was never built, much of the basic design is applicable. In particular, the translational motion drive system, controls system, stress analysis which included viscoelastic damping, structural design concepts, and attitude sensing systems are of particular interest.

LANGLEY RESEARCH CENTER STUDIES

The Langley Research Center's Lunar Landing Research Facility, known as the LLRF, is shown in Figure 4. The facility is designed to

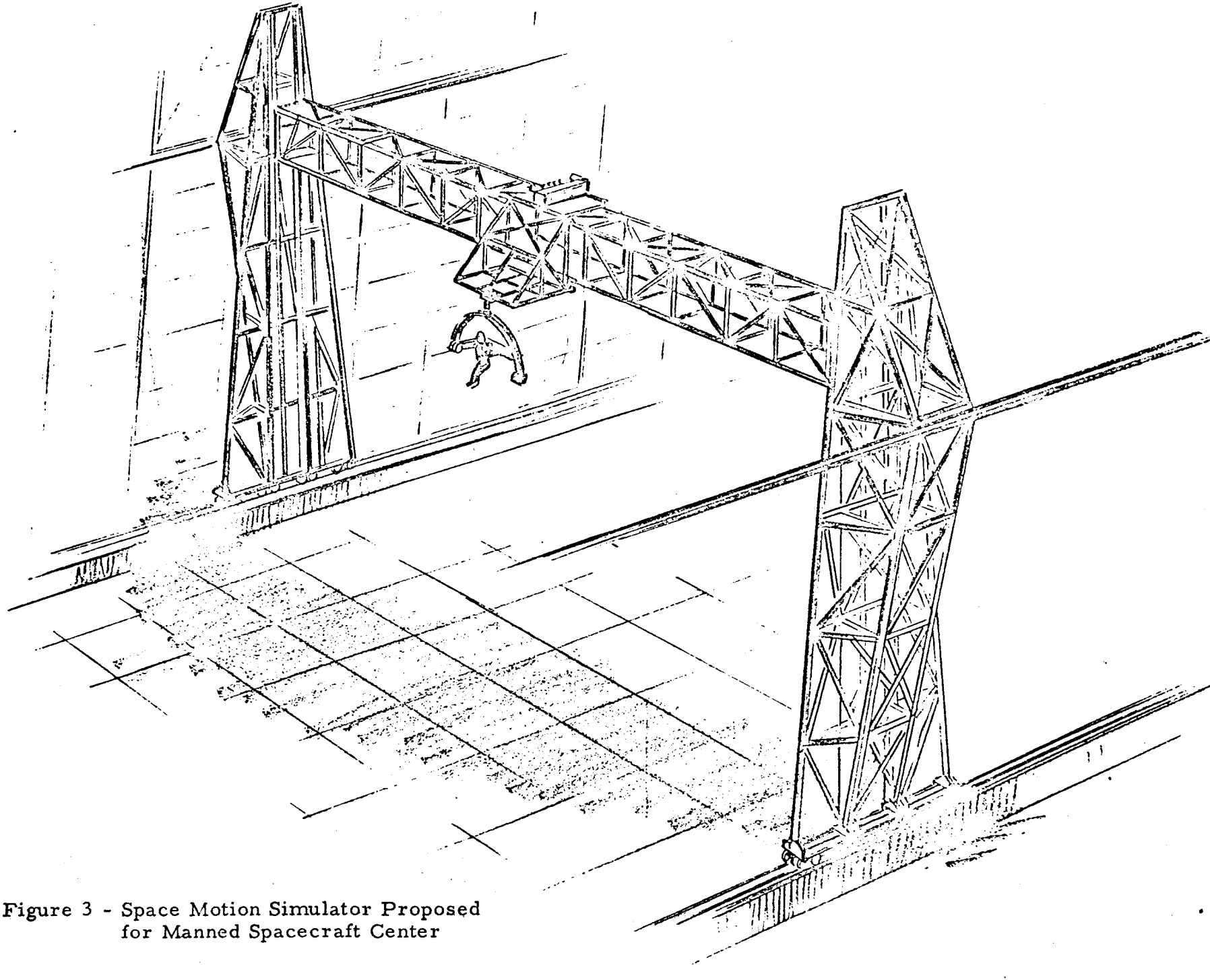

Figure 3 - Space Motion Simulator Proposed for Manned Spacecraft Center

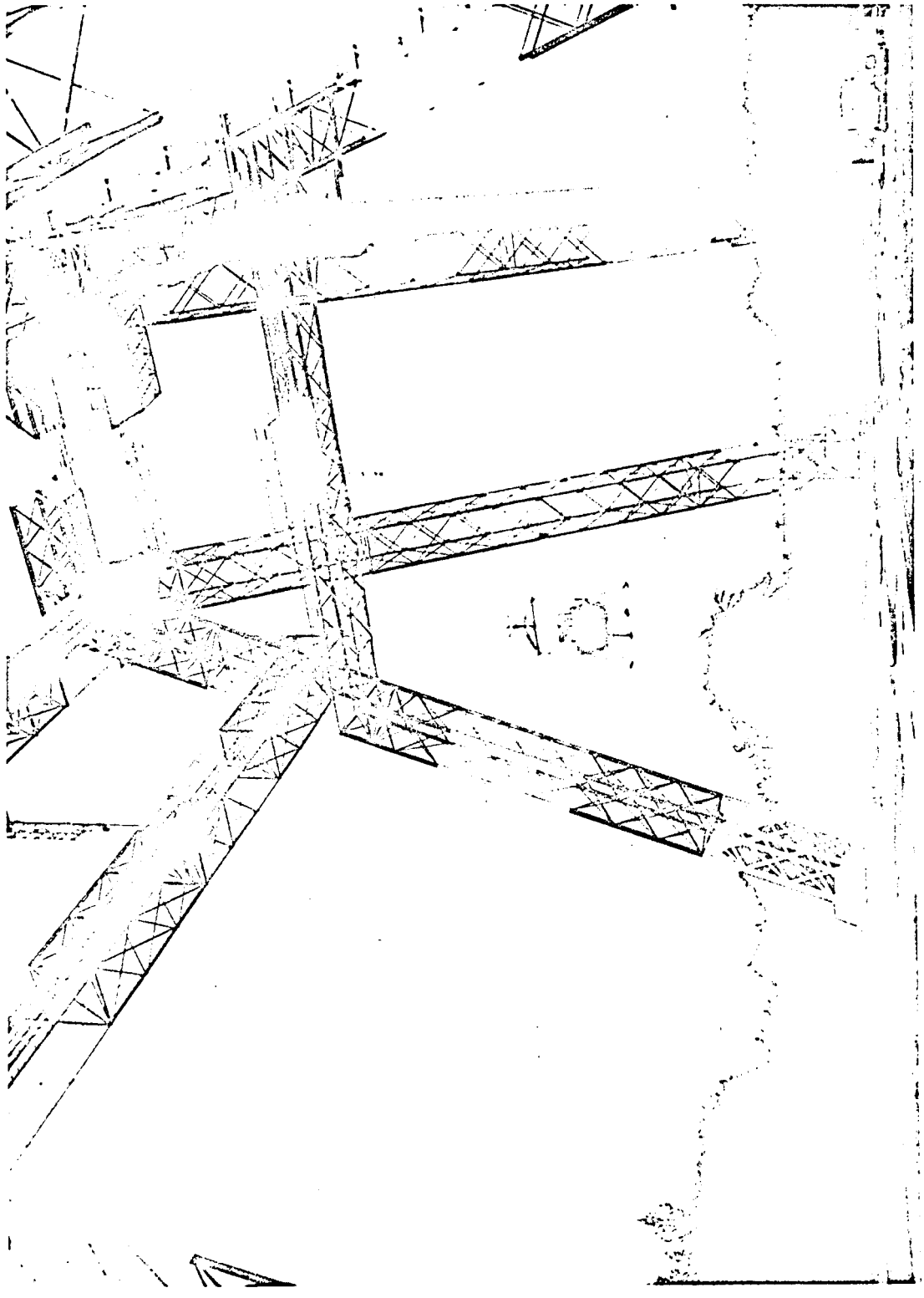

Figure 4 - Langley Lunar Landing Research Facility

permit lunar gravity landing tests of full-scale manned vehicles, but most have been conducted with a LEM mockup. Essentially, the facility consists of an overhead crane structure about 250 feet high, 60 feet wide and 400 feet long. The facility is capable of testing vehicles to 10,000 pounds. The crane supports 5/6 of the vehicle weight while the pilot controls attitude and rate of descent with the vehicle control system. The pilot has six-degrees-of-freedom within a volume 50 feet wide, 165 feet high and 400 feet long. However, the maximum vertical and longitudinal velocity and accelerations are much too low for application to the LGS program. Studies have been made to determine the costs of adapting this facility, and it was found to be much less expensive, as discussed in detail in Northrop Report E 30-80.

During the development of the simulator, a simplified mockup of the suspension system and flight vehicle was built and tested to check some of the ideas and systems to be used in the full scale simulator. The test vehicle was an open frame which carried the pilot. The vehicle was suspended inside a building by a cable from a ring 50 feet from the floor. A strain gauge supplies the input to a hydraulic motor winch to support 5/6 the vehicle weight. To keep the cable vertical, air driven winches were controlled by two operators. Thus, the pilot could "fly" within a 10-foot square area.

As a result of this survey, the following data will be of use in the design and analysis of a lunar gravity simulator.

From the Northrop reports, a background of lunar gravity simulator information was obtained, and a horizontal plane LGS was selected as the preferred concept. In addition, the use of any present facility in this program (particularly the Langley LLRF) was eliminated.

The study for Manned Spacecraft Center contributes: (1) the selection of hydraulics for rotary motions (high precision movements) and electrical motors for the translation system (lower precision movement); (2) the use of high natural frequency structure (approximately 5 times imposed

frequencies) rather than a low frequency, highly damped structure; (3) structural configurations with analysis for the crane system; and (4) harness systems which may be applicable for suspending the driver.

A winch-drive motor arrangement discussed in Langley Report TN D-2636 is similar to that planned for the LGS and will be directly applicable to this program.

Section 3

ANALYSIS AND SELECTION OF SUSPENSION DEVICE AND DRIVE SYSTEM CONCEPTS

Two of the major control problems for the Lunar Gravity Simulator System are the maintenance of a constant force in each of the suspension devices partially supporting the LSV's and the maintenance of vertical alignment at each LSV attachment point. The latter places a control burden on the trolley drive system and the vertical sensing mechanism. It is the objective of Task 1.3 of this study to determine a workable solution to this control problem and to recommend specifications for key suspension devices and drive system components.

The first phase of efforts on this task has been directed toward establishing the suspension device configuration, deriving mathematical expressions for force control mechanisms, and analyzing techniques for sensing the LGS trolley and LSV relative positioning. The approaches which are recommended for further investigation are:

1. 1/6 g suspension of the LSV should consist of independent suspension devices attached to each of the key LSV attachment points (two for chassis and one each for each wheel, for instance) and each device should be attached to a suspension platform on an overhead trolley.
2. Servo-controlled hydraulic rotary motors appear to be logical choices for the force control mechanisms. Also, hydraulic motors appear to be a likely candidate for the trolley drive motors. Alternates should include an ironless disc electric motor which has a momentary overload capability of up to 25:1.
3. An optical sensing technique for the trolley positioning system appears to be the most desirable approach of four systems considered. This system involves a light source and photovoltaic sensing device which detects relative lateral displacement of the trolley and LSV via a light beam reflected from a corner reflector mounted on the LSV.

The following paragraphs describe the background for the recommendations listed above.

REQUIREMENTS

Static and Dynamic Accuracy

The prime objective of the suspension system is to support 5/6 of the weight on earth of the test vehicle as precisely as possible during all realistic maneuvers. The most severe requirements are encountered when the vehicle is driven at maximum speed on rough terrain.

This results in high displacement rates and accelerations of the suspended parts. The following requirements that should be met by the suspension system were derived from various sources.

Deviations from the nominal weight to be suspended F_o shall be

$$f = \frac{F - F_o}{F_o} \leq 10\%$$

This accuracy should be maintained under the following conditions:*

$$\ddot{Z}_{\text{wheel hub}} \leq 4\ g_{\text{earth}}$$

$$\dot{Z}_{\text{wheel hub}} \leq 30 \text{ ft/sec } (9.1 \text{ m/sec})$$

$$\ddot{Z}_{\text{main vehicle}} \leq 0.5\ g_{\text{earth}}$$

$$\dot{Z}_{\text{main vehicle}} \leq 10 \text{ ft/sec } (3 \text{ m/sec})$$

Weight

In addition, the total suspension system must be of minimum weight because the system must be supported by the upper trolley system. The trolley system must closely follow the fore and aft motions of the vehicle. Overall weight of the moving trolley should, therefore, be kept to a minimum.

*Preliminary maximum values

Ease of Operation and Calibration

Efficient utilization and operation of the LGS for testing a variety of different vehicles implies that the suspension system can be adapted to different test articles and calibrated to changing weights, payloads or drives in the shortest possible time.

Weighing the Test Vehicle

Before the system is calibrated, it is desirable that the suspension system be used to determine the actual earth weight of each suspended part. As will be discussed in subsequent paragraphs, there are suspension concepts that offer convenient ways to weigh the vehicle at all supported points in minimum time. The weighing mode can be mechanized with a small amount of additional hardware.

SELECTION OF SUSPENSION SYSTEM CONCEPT

The basic concept for the Lunar Gravity Simulator (LGS) consists of a suspension platform rigidly attached to an overhead trolley. The suspension system consisting of a cable network and force control system links the Lunar Surface Vehicle (LSV) to the suspension platform. Suspension system concepts have varied from direct cables between the suspension platform (and force controller) and the LSV to systems having harness arrangements, hydraulic or pneumatic cylinders, negator springs, and similar items as intermediate components between the cable and the LSV attachment point. Some of these arrangements incorporated harness mechanisms hanging from the primary support cable and supporting the wheel masses with negator springs. A survey of these configurations led to the following dynamic analysis to evaluate the effects of the varied arrangements.

Effects of Cable Length on Dynamic Performance

The free length of the suspension cables affects the LGS performance mainly in two different ways depending upon the direction of the disturbing forces:

1. Longitudinal Cable Dynamics after Vertical Disturbances

The longitudinal cable dynamics are dominated by the spring constant of the cable

$$K_c = \frac{E A_c}{L} \tag{1}$$

where

E Young's modulus of cable material

A_c cross sectional area of cable

and by the interactions of the constant force device and the cable (Figure 4). The time for longitudinal stress wave propagation is

$$t_L = \frac{L}{C_L} \tag{2}$$

where C_L is the longitudinal stress wave propagation velocity (equal speed of sound in cable material). For a steel cable of 33 feet (10 m)

$$t_\ell \approx \frac{10}{5000} = 0.002 \text{ sec}$$

Therefore, t_ℓ can usually be neglected.

In order to study the effects of cable length L it will be assumed that a step type displacement $Z_1(S) = Z_{10}/S$ occurs at the low end of the cable. The resulting transient of the cable force F is obtained with the help of the transfer function of the constant force device (CFD) derived in a later

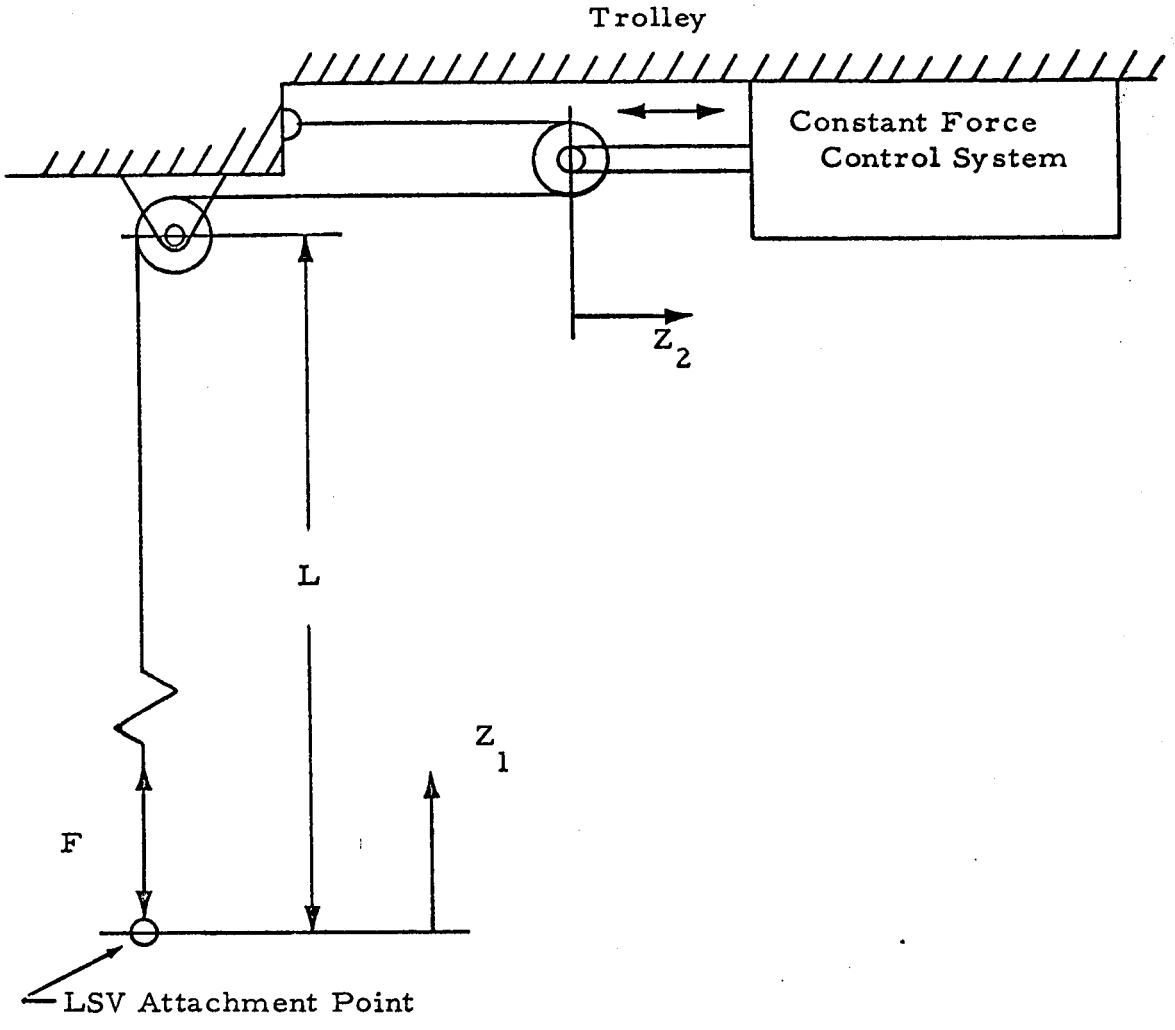

Figure 5 - Longitudinal Cable Dynamics

section. Neglecting higher-order modes the CFD is approximately described by

$$\frac{F(S) - F_o}{Z_2(S)} = -K \frac{S}{TS+1} \approx -KS \qquad (3)$$

where F_o is the nominal cable force, K and T are constant CFD parameters. Combining Equation (3) with the cable spring equation

$$F - F_o = K_c(Z_2 - Z_1) \tag{4}$$

yields the first-order transfer function

$$F - F_o \approx \frac{KS}{\frac{K}{K_c}S + 1} Z_1(S)$$

For the step deflection $Z_1 = Z_{10}$ the time response of Figure 6 is obtained with a peak at t = 0

$$(F - F_o)_{peak} \approx - K_c Z_{10} = - \frac{EA_c}{L} Z_{10}$$

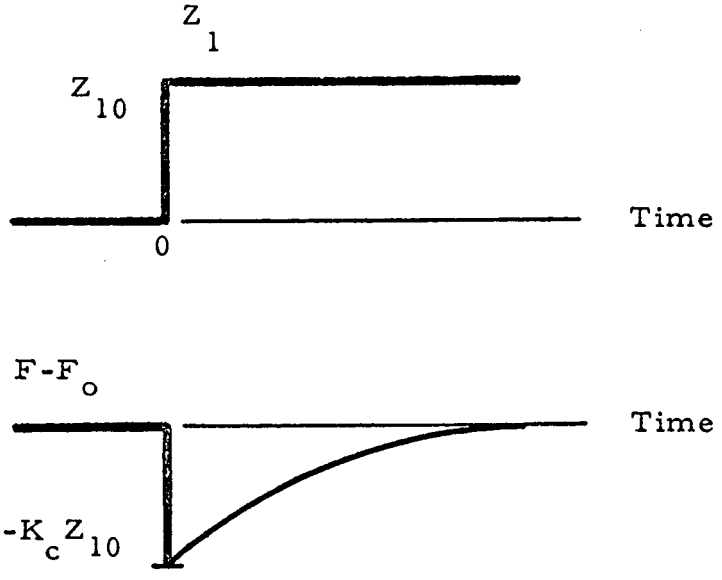

Figure 6 - Approximate Error in Cable Tension F due to Step Disturbance

This shows that peak errors in the longitudinal cable dynamics are a minimum for maximum cable length and minimum cable diameter.

2. Transversal Cable Dynamics after Horizontal Disturbances

As was outlined in detail in Section 3.3 of the proposal, horizontal disturbances of the vehicle motion as caused by surface obstructions accelerating or decelerating the vehicle impose a serious burden on the trolley drive and suspension system.

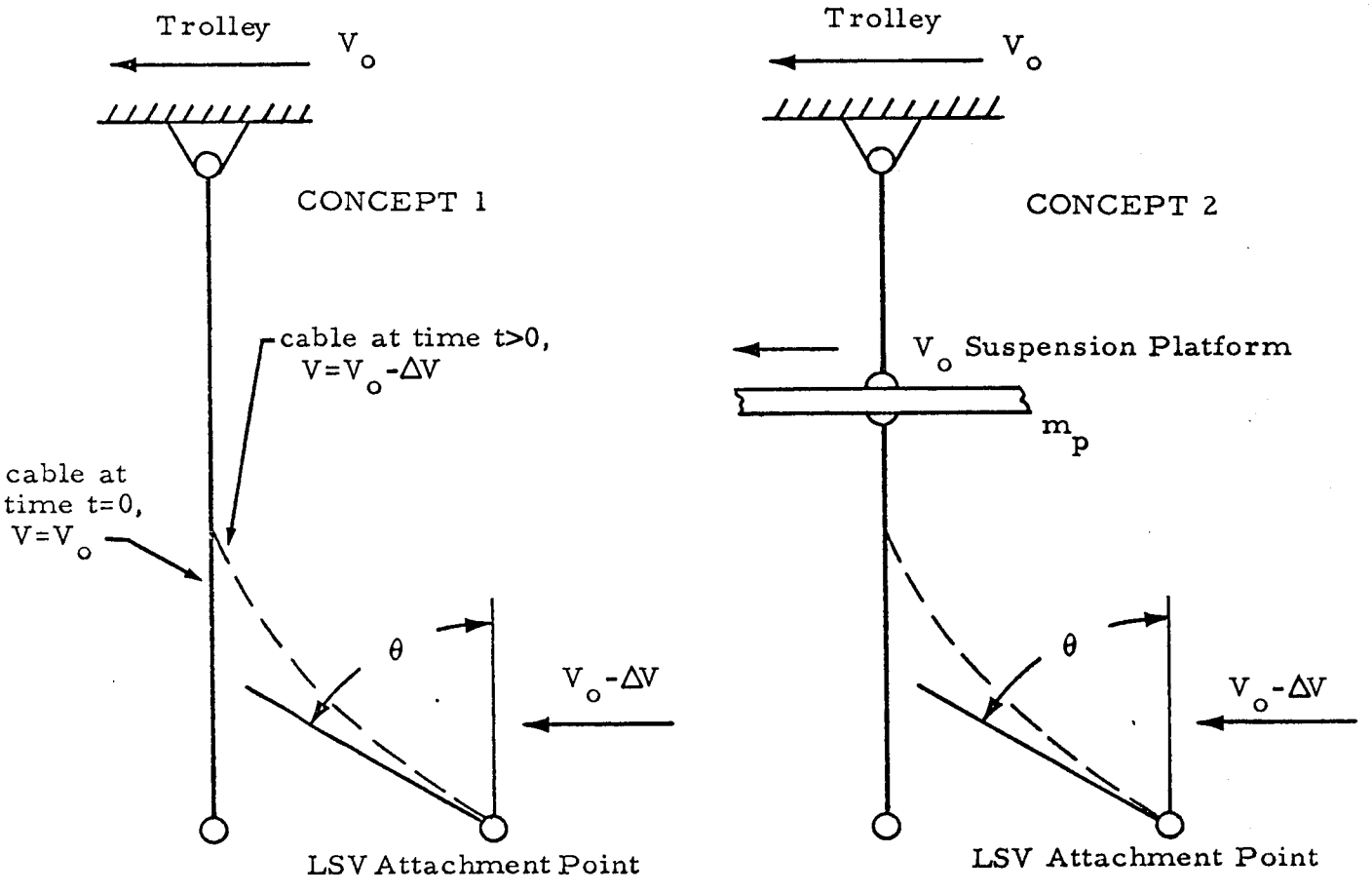

Figure 7 - Suspension Cable Transversal Perturbation for Concept 1 and Concept 2

As shown in Figure 7, a velocity increment ΔV due to a horizontal perturbation causes an initial cable misalignment

$$\theta \approx \frac{\Delta V}{C_T} \tag{5}$$

and a horizontal driving force error

$$F_H \approx F_o \sin\theta \tag{6}$$

to the LSV, where F_o is the nominal cable tension and C_T is the transversal wave propagation velocity

$$C_T = \sqrt{F/\zeta A_c} \quad (\zeta = \text{cable material density}) \tag{7}$$

As is readily seen from Figure 7 and Equations 5 through 7, this driving force error is not dependent on the cable length, whereas the time t_T required for the trolley to respond to the angular error is proportional to cable length but cannot be reduced by lowering the suspension platform as in concept 2. The need for aligning the low suspension platform in addition to the trolley after a horizontal perturbation even deteriorates the performance.

Summarizing these results led to suspension platform concept 1 (direct cable) as the preferred choice.

SELECTION OF CONSTANT FORCE CONTROL SYSTEM

Various ways to keep the cable tension at the nominal value have been considered. These include cable winches driven by electric dc servomotors, ironless disc electric servo motors with various types of clutches, mechanical negator springs to control the cable tension and electro-pneumatic and electro-hydraulic servo systems to drive constant torque winches or linear actuators controlling cable tension. A brief summary of the comparison and the factors considered is shown in Figure 8. As all preliminary control studies indicate that precise control of the trolley drive system is one of the

Component / Characteristic	Electric Motor (with clutch)	Ironless Elect. Motor (with clutch)	Negator Springs	High Pressure Pneumatic Cylinder	Hydraulic Motor (constant torque winch)
Force Sensor	Load Cell	Load Cell	None	Pressure Transducer	Load Cell
Static Accuracy	○ ○ ○	○ ○ ○	○ ○	○ ○ ○	○ ○ ○
Dynamic Accuracy	high inertia ○	med. inertia ○ ○	high inertia; danger of buckling; open loop; no soft spring filtering ○	Compressibility effects ○ ○	low inertia ○ ○ ○
Weight/Power Ratio	○	○ ○	○	○ ○ ○	○ ○ ○
Ease of Force Adjustment and Calibration	○ ○ ○	○ ○ ○	Suspension system must be changed or modified ○	○ ○ ○	○ ○ ○
Cost	○ ○ ○	○ no stock production	○ ○ ○	○ Expensive high pressure air supply	○ ○
Space/Power Ratio	○	○	○ ○ ○	○ ○ more ancillary equipment req'd	○ ○ ○
Availability of Components on Market	○ ○ ○	Designed and built to customer's specif. ○	○ ○ ○	○ ○	○ ○ ○

Best Choice

○ ○ ○ Excellent
○ ○ Fair
○ Poor

Figure 8 - Comparison of Constant Force Control System Components

most critical areas, most weighting was given to minimum weight of those components of the system that are mounted on the trolley. The electro-hydraulic servo system with feedback controlled constant torque winch motor and with cable force sensors at the lower cable ends was found optimum. The system is described and analyzed in the next section.

CONSTANT FORCE CONTROL SYSTEM ANALYSIS

The basic configuration of the constant force control system is shown in Figure 9. A hydraulic motor drives a low inertia cable winch. The valve monitoring the winch is a high performance pressure control servo valve. The cable tension close to the LSV attachment point is sensed by a pressure transducer. In a LGS control and calibration console, the cable force signal is compared with the nominal value. The resulting error signal is shaped in a lead-lag compensating network and then fed into the servo valve. A typical calibration sequence prior to LSV tests with the LGS may be as follows:

1. Adjust pots for primary chassis support point until recommended 1/6 g vehicle suspension system deflections* are reached.
2. Adjust pots for each wheel support point until static wheel deflections* for 1/6 g are reached.

The closed-loop dynamics can be derived from the block diagram of Figure 10. A first approach was made by assuming a compensating network with transfer function

$$G_N = 1.$$

Neglecting the dither signal i_d which is applied to reduce stick-free friction effects an overall transfer function for the closed-loop of the form

$$\left(f = \frac{F - F_o}{F_o} = \text{normalized force error}\right)$$

*These deflections are determined by previous vehicle weight calibrations.

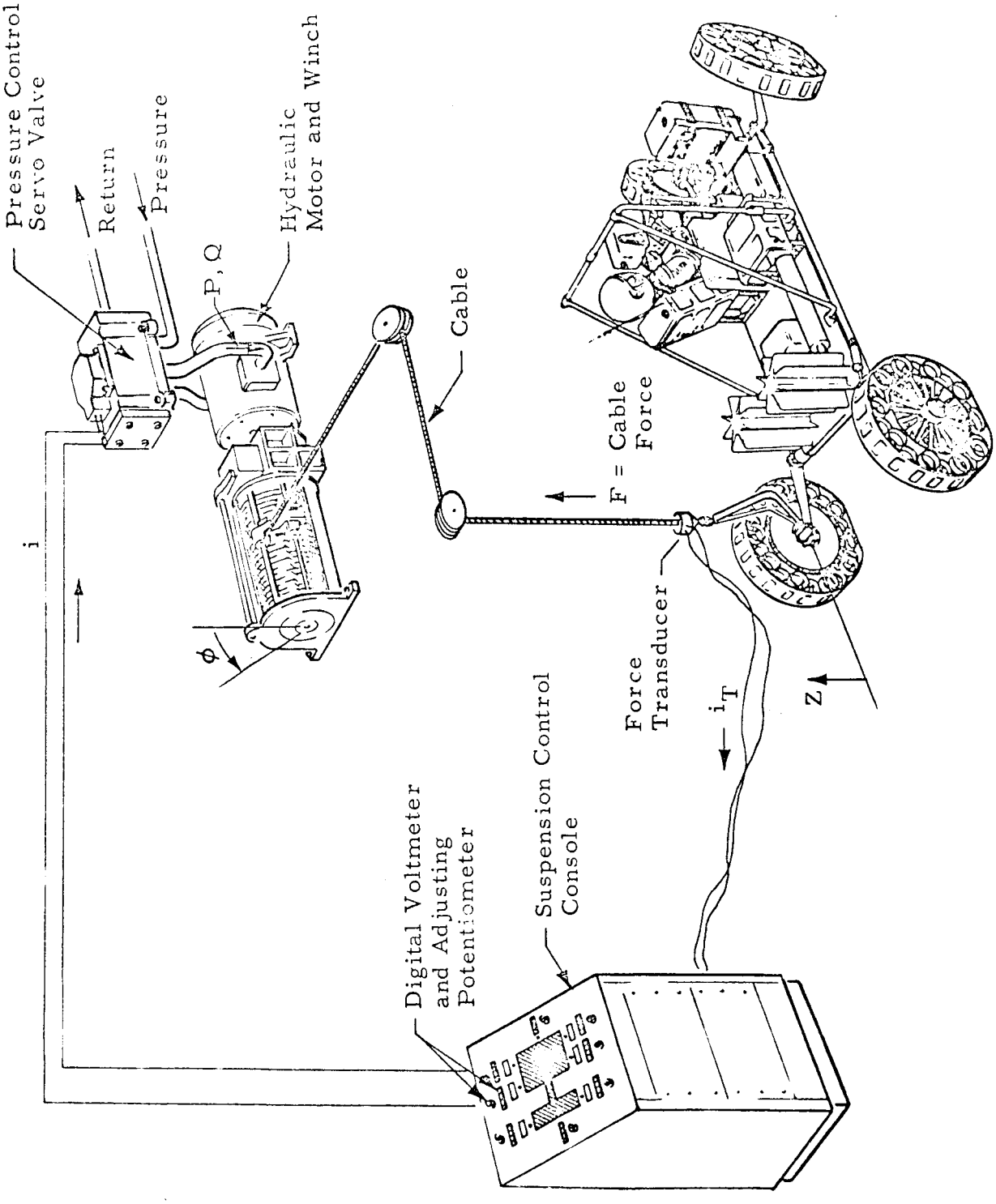

Figure 9 - Basic Configuration of Constant Force Control System (Schematic)

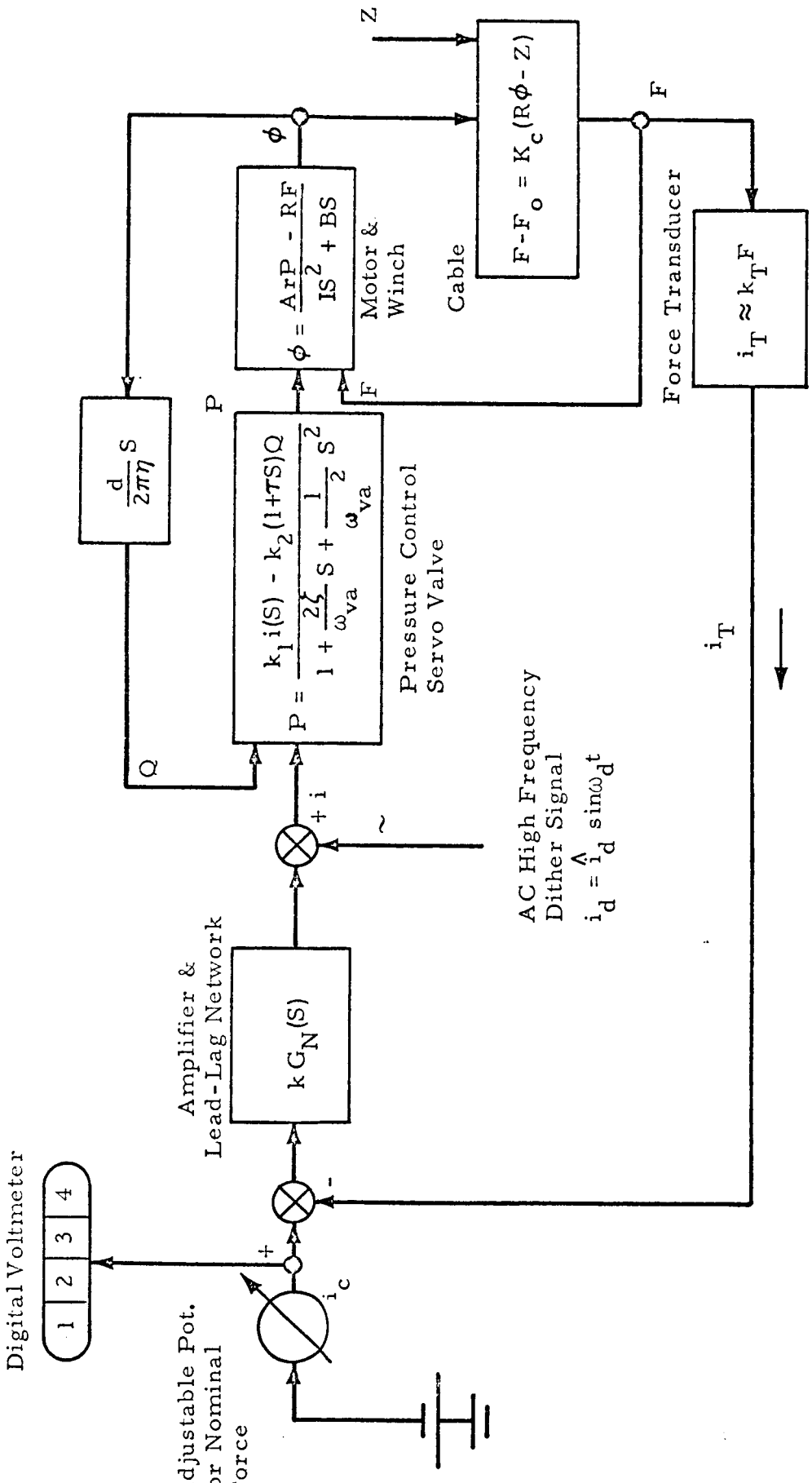

$$\frac{f(S)}{\dot{Z}(S)} = -\frac{K_c}{F_o} \frac{A_1S^3 + A_2S^2 + B_3S + B_4}{A_1S^4 + A_2S^3 + A_3S^2 + A_4S + A_5}$$

Figure 2.1 - Block Diagram of Constant Force Control System

$$\frac{f(S)}{Z(S)} = - \frac{K_c}{F_o} \frac{A_1 S^3 + A_2 S^2 + B_3 S + B_4}{A_1 S^4 + A_2 S^3 + A_3 S^2 + A_4 S + A_5} \tag{8}$$

is obtained with the coefficients

$$A_1 = \frac{I P_o}{T_o \omega_v^2} \left[\frac{\text{lb sec}^4}{\text{ft}^2}\right]$$

$$A_2 = \frac{P_o}{T_o \omega_v} \left(2\zeta I + \frac{B}{\omega_v}\right) \left[\frac{\text{lb sec}^3}{\text{ft}^2}\right]$$

$$A_3 = \frac{P_o}{T_o} \left(I + \frac{2B\zeta}{\omega_v} + \frac{K_c R^2}{\omega_v^2}\right) + \frac{k_2 \tau d}{2\pi\eta} \left[\frac{\text{lb sec}^2}{\text{ft}^2}\right]$$

$$B_3 = \frac{P_o}{T_o} \left(I + \frac{2B\zeta}{\omega_v}\right) + \frac{k_2 \tau d}{2\pi\eta} \left[\frac{\text{lb sec}^2}{\text{ft}^2}\right]$$

$$A_4 = \frac{P_o}{T_o} \left(B + \frac{2\zeta K_c R^2}{\omega_v}\right) + \frac{k_2 d}{2\pi\eta} \left[\frac{\text{lb sec}}{\text{ft}^2}\right]$$

$$B_4 = \frac{B P_o}{T_o} + \frac{k_2 d}{2\pi\eta} \left[\frac{\text{lb sec}}{\text{ft}^2}\right]$$

$$A_5 = K_c R \left(\frac{P_o}{F_o} + k\, k_1\, k_T\right) = k_3\, K_c\, R \left[\frac{\text{lb}}{\text{ft}^2}\right]$$

are defined in Reference 1, pages 24 and 24, where the parameters are:

I = the moment of inertia of motor and winch and cable
P_o = the nominal hydraulic pressure
T_o = the nominal hydraulic motor torque
F_o = the nominal cable force
ω_v = valve natural frequency

ζ = the valve damping constant

B = the viscous damping in the motor

K_c = EA_c/L_c where E is Young's modulus, A_c is the cross sectional area of cable, and L_c is the cable length

R = the effective winch radius

τ = the valve droop time constant

d = the volumetric displacement of motor per revolution

η = the volumetric efficiency of motor

k_T = the force transducer constant

k_1 = valve constant

k_2 = the valve static droop constant

k_3 = $P_o/F_o + k\,k_1\,k_T$, is the adjustable loop gain

Neglecting the motor and winch inertia I and viscous damping B results in the second-order approximation

$$\frac{f(S)}{\dot{Z}(S)} = -k\,\frac{1}{E_1S^2 + E_2S + 1}$$

which was used for the preliminary analog simulations presented in the section entitled, "LSG Sample Analog Output Data".

The optimum compensating network for the complete system will be determined by a root-locus synthesis.

TROLLEY POSITIONING SYSTEM

Support cables between the trolley and LSV must remain vertical at all times in order to minimize horizontal forces exerted on the LSV through the cables. To maintain vertical cables, the trolley must remain in a fixed position relative to the LSV. Two basic methods have been proposed to maintain this constant relative position:

1. Detect variations of the cables from the vertical and drive the trolley to compensate.

2. Detect relative horizontal movement between a point on the trolley and the c.g. of the LSV; again compensate by driving the trolley.

A potentiometer, mounted on the trolley, with a feeler arm riding the cable (Figure 11a) has been proposed as a means of detecting cable deviation from the vertical. The primary disadvantage of this method is in dealing with the problems caused by the whip-lash or vibrating spring motion of the cable. This cable motion may add considerable error and instability to the trolley positioning system. Use of an angle potentiometer for the detector would likely require a filtering network which would compromise the overall system accuracy.

The relative horizontal movement may be detected by an audio position indicator (Figure 11b) which operates on the sonar principle. A 30 KHz audio signal is transmitted at the c.g. of the LSV. This signal travels at 1100 ft/sec (speed of sound in air) in all directions and audio receivers (microphones) at each end of the trolley pick up the signal. If one mic is closer to the transmitter than the second mic, the first mic will pick up the signal before the second. The time between the microphone pick-ups is a measure of the error signal generated. The trolley may be driven until signals arrive at both microphones simultaneously, indicating that the trolley is directly over the c.g. Problems may arise in this type system due to sound waves traveling from the LSV through the cables to the trolley microphones at a speed greater than the speed of sound in air.

Relative horizontal movement between trolley and LSV may also be detected by optical means. Optical detectors mounted on the trolley may either:

- sense angular displacement of a light beam directed to the LSV and reflected back to the trolley by a reflector mounted in line with the c.g. of the LSV; or

- sense relative horizontal movement of an LSV mounted corner reflector* with respect to a collimated light source fixed to the trolley (Figure 12).

A star tracker with a collimated light source mounted on top of the tracker may be used to follow a reflector mounted along the line of c.g. of the LSV. Angular movement of the star tracker may be measured to provide a vertical error signal. A servo system may be used to maintain the star tracker perpendicular to the trolley by moving the trolley until the reflector is directly below the star tracker. However, this system requires additional servo loops over a horizontal displacement system such as the photovoltaic system in Figure 12 and was eliminated from further consideration.

The photovoltaic** system (Figure 12) consists of a fixed collimated light source on the trolley with a fixed photosensitive null indicator beside the light source and a corner reflector mounted on the LSV, along the line of c.g. As the corner reflector moves into and out of the light beam, the photovoltaic null indicator senses the changes in intensity of reflected light. The trolley will be moved to maintain equal light intensities in both photo diodes of the null indicator and therefore keep the trolley directly above the corner reflector.

---

* Corner reflector: A corner reflector consists of three mirrors mounted perpendicular to each other. Light beams transmitted to and reflected from the corner reflector are always parallel independently of the orientation of the corner reflector. In our particular application, the light beam reflected back toward the trolley will be parallel to the beam transmitted from the trolley independently of the LSV pitch and roll.

** Photovoltaic null indicator: A dual element photovoltaic null indicator consists of two photo-diodes mounted side by side. When the indicator is used with a balanced amplifier, the difference in light intensity upon the two diodes can be determined. In our particular application, the diodes, equally spaced from the center of the collimated light source, can be used to indicate the horizontal displacement of the corner reflector relative to the light source.

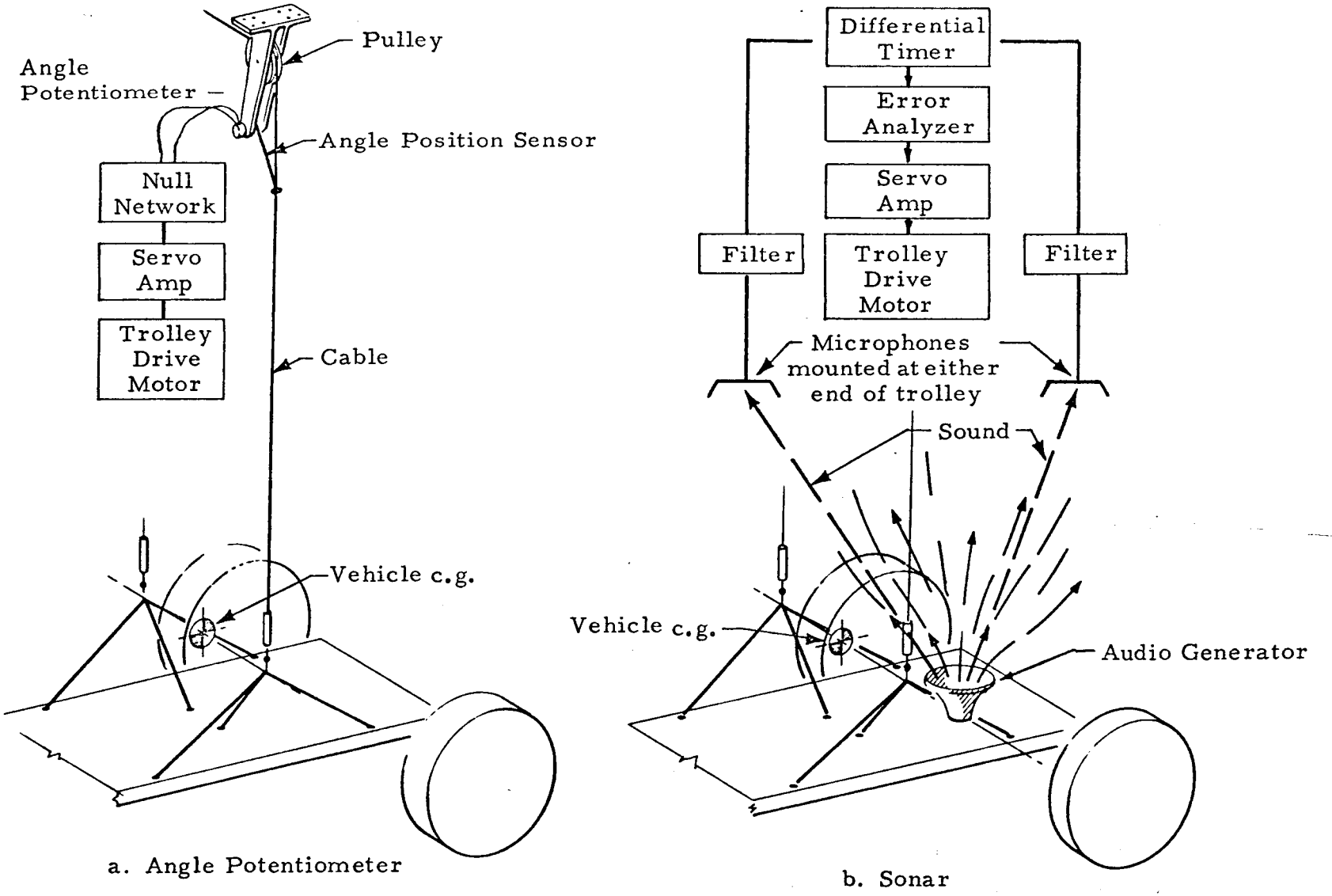

Figure 11 - Trolley Positioning System

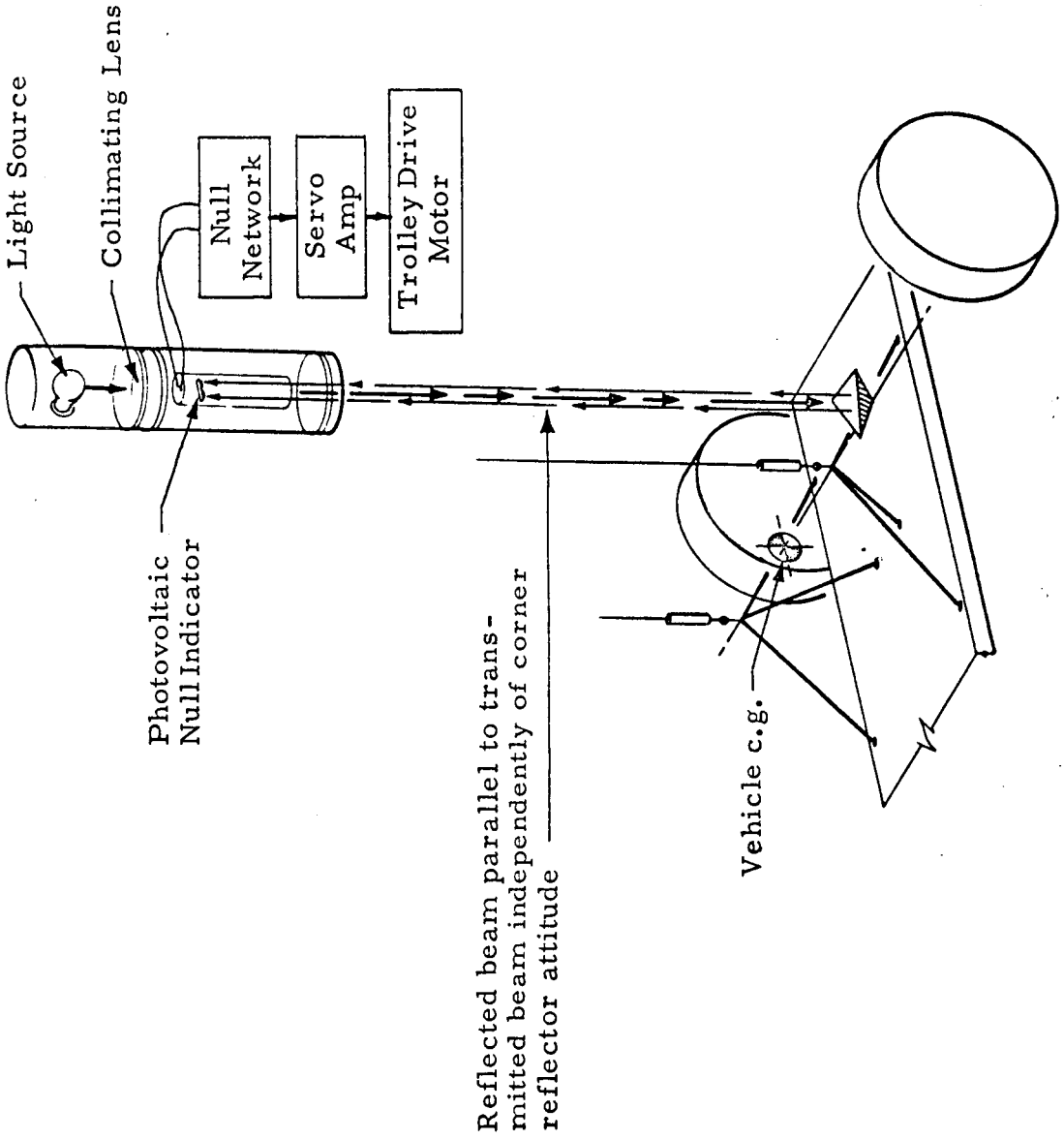

Figure 12 - Photovoltaic Trolley Positioning System

Figure 13 compares the three trolley positioning systems currently under study. The angle potentiometer provides the least expensive and most straightforward of the three positioning systems. Except for a possible accuracy problem, this would be a logical first choice because of its simplicity. Analysis indicates the long response time of this system will probably allow too much cable angle error. In order to reduce this response time, the sensor used should detect errors in cable angle or trolley position at the LSV rather than at the trolley. Locating an angle sensor at the LSV loses the vertical reference available at the trolley suspension platform.

The three systems which detect horizontal movement of the c.g. of the vehicle with respect to the trolley have been analyzed. The photovoltaic system is believed to be the superior of the three. The sonar system has not been analyzed in detail, but preliminary studies indicate that sound traveling through the cables at a speed greater than the velocity of sound in air will add isolation problems to the microphone design.

The photovoltaic null indicator will rapidly indicate the position of the trolley with respect to the LSV. The instrument can be mounted on the trolley with only a corner reflector mounted on the LSV. The cost is moderate and the problems seem to be minimum. If further analysis indicates that the required response is too rapid for the angle potentiometer, the photovoltaic system seems to satisfy all requirements at a cost which is reasonable, even though it is greater than the cost of the potentiometer system. It is recommended that both the angle potentiometer and the photovoltaic concepts be evaluated with the trolley drive system analog simulation.

System	Angle Potentiometer	Photovoltaic	Sonar
Operation			
Precision	One degree	4 minutes or better	One minute
Vibration Sensitivity	Sensitive to cable & trolley vibration	Sensitive to trolley vibrations	Slightly sensitive to trolley vibrations
Noise Sensitivity	Relatively insensitive	Sensitive to certain frequencies of stray light	
Vehicle Interface	No problem	Corner reflector must be mounted along axis of c.g.	Audio generator output must be mounted along axis of c.g.
Relative Availability	Off the shelf	Some development	Development required
Relative Cost	Low cost	Moderate cost	Expensive
Problem Areas	Cable vibrations Slow response	Simpler Photo System	Audio signal traveling through cables

Figure 13 - Comparison of Trolley Positioning Systems

Section 4

IDENTIFICATION OF TEST PARAMETERS AND ESTABLISHMENT OF LGS/LSV MATHEMATICAL MODEL

The results of this task will be an engineering tool for evaluating the two-dimensional Lunar Gravity Simulator System. Study efforts during this reporting period resulted in (1) the establishment of test parameters representing maximum lunar terrain conditions; (2) identification of pertinent LSV mobility characteristics for evaluating the LGS; (3) derivation of wheel input relationships for traversing simulated obstacles, and (4) derivation of a LGS/LSV mathematical model for simulation on an analog computer. These results are discussed in the following paragraphs.

TEST PARAMETERS

The test parameters to identify are the obstacle and slope combinations which represent maximum terrain conditions for the Lunar Surface Vehicles. Typical worst obstacles which may be used in combination with maximum terrain slopes up to 35 degrees are shown below.

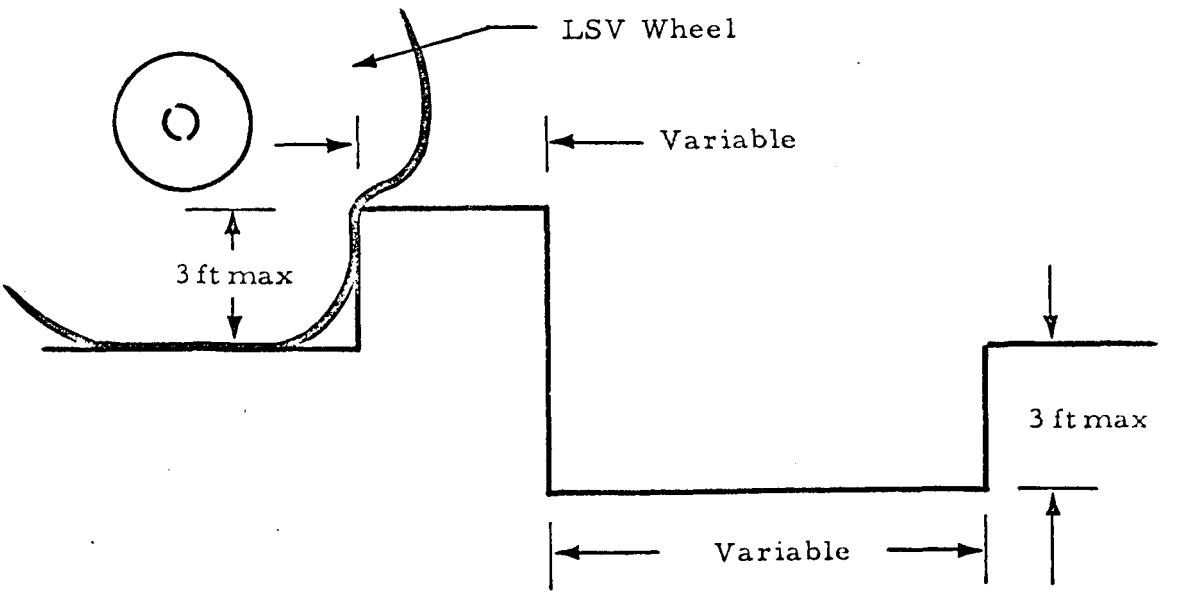

These obstacles will be used as inputs to an analog computer simulation of the two-dimensional Lunar Surface Vehicle (LSV) and the gravity simulator system. The simulation involves the LSV wheels encountering obstacles at forward velocities sufficient to affect the following loading conditions:

Transient

Wheel vertical acceleration $\pm$ 128.8 ft/sec^2

Steady State (Chassis cg) RMS values

Vertical	$\pm$ 8.3 ft/sec^2
Pitch	$\pm$ 1.6 rad/sec^2
Roll	$\pm$ 2.3 rad/sec^2

Obstacle/velocity combinations which cause these loading conditions will be used in conjunction with typical LSV's to establish the motion characteristics at key suspension device attachment points. The horizontal perturbations caused by these loading conditions will establish the steady state and transient drive system characteristics for the LGS trolley system supporting the LSV.

MOBILITY CHARACTERISTICS OF LUNAR SURFACE VEHICLES

Two primary vehicles have been chosen for use in establishing the design characteristics for the LGS. These are the MOLAB and LSSM vehicles which have been under study by Bendix Corporation and the Boeing Company. Because of the recent emphasis on the LSSM vehicle, it was chosen for evaluation first. The Bendix LSSM Mobility System characteristics which are representative of the data required for evaluation with the LGS are tabulated in Table 1. Similar data for other vehicles are presently under study or have been requested from NASA.

Table 1*

PARAMETERS	DESCRIPTION	UNITS
K_1 = 457.2	Wheel Spring Constant	lb/ft
K_2 = 457.2	Wheel Spring Constant	lb/ft
K_3 = 272.2	Wheel Spring Constant	lb/ft
K_4 = 304.8	Wheel Spring Constant	lb/ft
K_5 = 181.2	Suspension Spring Constant	lb/ft
K_6 = 272.2	Suspension Spring Constant	lb/ft
K_{15} = 2860	Cable Spring Constant	lb/ft
K_{18} = 296	Cable Spring Constant	lb/ft
K_{19} = 296	Cable Spring Constant	lb/ft
K_{13} = 296	Cable Spring Constant	lb/ft
K_{14} = 296	Cable Spring Constant	lb/ft
K_{16} = 2860	Cable Spring Constant	lb/ft
K_{11} = 28,800	Inner-Wheel Spring Constant	lb/ft
K_{22} = 28,800	Inner-Wheel Spring Constant	lb/ft
K_{33} = 28,800	Inner-Wheel Spring Constant	lb/ft
K_{44} = 28,800	Inner-Wheel Spring Constant	lb/ft
D_3 = 93.6	Suspension Damping Constant	lb-sec/ft
D_5 = 62.4	Suspension Damping Constant	lb-sec/ft
D_6 = 93.6	Suspension Damping Constant	lb-sec/ft
X_1 = 5.3	c.g. to Front Wheel	ft
X_2 = 7.5	c.g. to Front Wheel	ft

NOTE: Data in this table were obtained from the NASA/MSFC Astrionics Laboratory, Advanced Studies Branch, Mr. George Neal (876-9542)

Table 1 (Cont'd)

PARAMETER	DESCRIPTION	UNITS
$Y_1 = 3.42$	c.g. to Left Wheel	ft
$Y_2 = 3.42$	c.g. to Right Wheel	ft
$I_X = 373.3$	Moment of Inertia (X Axis)	Slug-ft^2
$I_Y = 475.0$	Moment of Inertia (Y Axis)	Slug-ft^2
$M_1 = 2.48$	Wheel Mass	Slugs
$M_2 = 2.48$	Wheel Mass	Slugs
$M_3 = 2.48$	Wheel Mass	Slugs
$M_4 = 2.17$	Wheel Mass	Slugs
$M_T = 62.11$	Total Body Mass	Slugs
$M_5 = 36.35$	Effective Body Mass (Roll)	Slugs
$M_6 = 31.05$	Effective Body Mass (Pitch)	Slugs
$g_E = 32.172$	Earth Gravity	ft/sec^2
$g_L = 5.362$	Lunar Gravity	ft/sec^2
$S_{1-4} = 0.583$	Displacement Before Wheel Snubbing	ft
$S = \pm 1.000$	Displacement Before Suspension Bottoming	ft

WHEEL GEOMETRY AND MOTION MECHANICS

The dynamics of a wheel hitting an obstacle can be described realistically in two phases, as shown in Figure 14. The inner wheel is assumed rigid. Therefore, the results are slightly worse than actual forces:

- Phase I ($0<t<t_1$): From touching the obstacle at t=0 to $t=t_1$, when the outer rim and springs bottom on the inner wheel frame. Force acting from edge of obstacle toward center of wheel increases according to wheel spring characteristic:

$$t_1 = \frac{R - r}{V \cos\alpha(H)}, \tag{1}$$

$$\alpha(H) = \sin^{-1} \frac{r_{sT} - H + Z_1^{(0)}}{r}$$

$$F_V = (K_1 V t + K_2 V^2 t^2) \sin\alpha(H) \tag{2}$$

Disturbance (1) results in displacement of wheel hub computed by analog computer:

$$Z^{(1)}(t_1) = Z_1^{(1)}.$$

$Z_1^{(1)}$ is compared with estimated value $Z_1^{(0)}$ in Equation (1). If necessary, the computation is repeated with a better estimate until

$$Z_1^{(\eta)} \approx Z_1^{(\eta-1)}.$$

- Phase II ($t_1<t<t_2$): After outer wheel springs bottom at edge of obstacle: The wheel hub is displaced along approximately a sinusoidal trajectory with vertical velocity

$$\dot{Z}(t) = V \cot\alpha(H) \cos \frac{\pi V}{2r \cos\alpha(H) + L} t \tag{3}$$

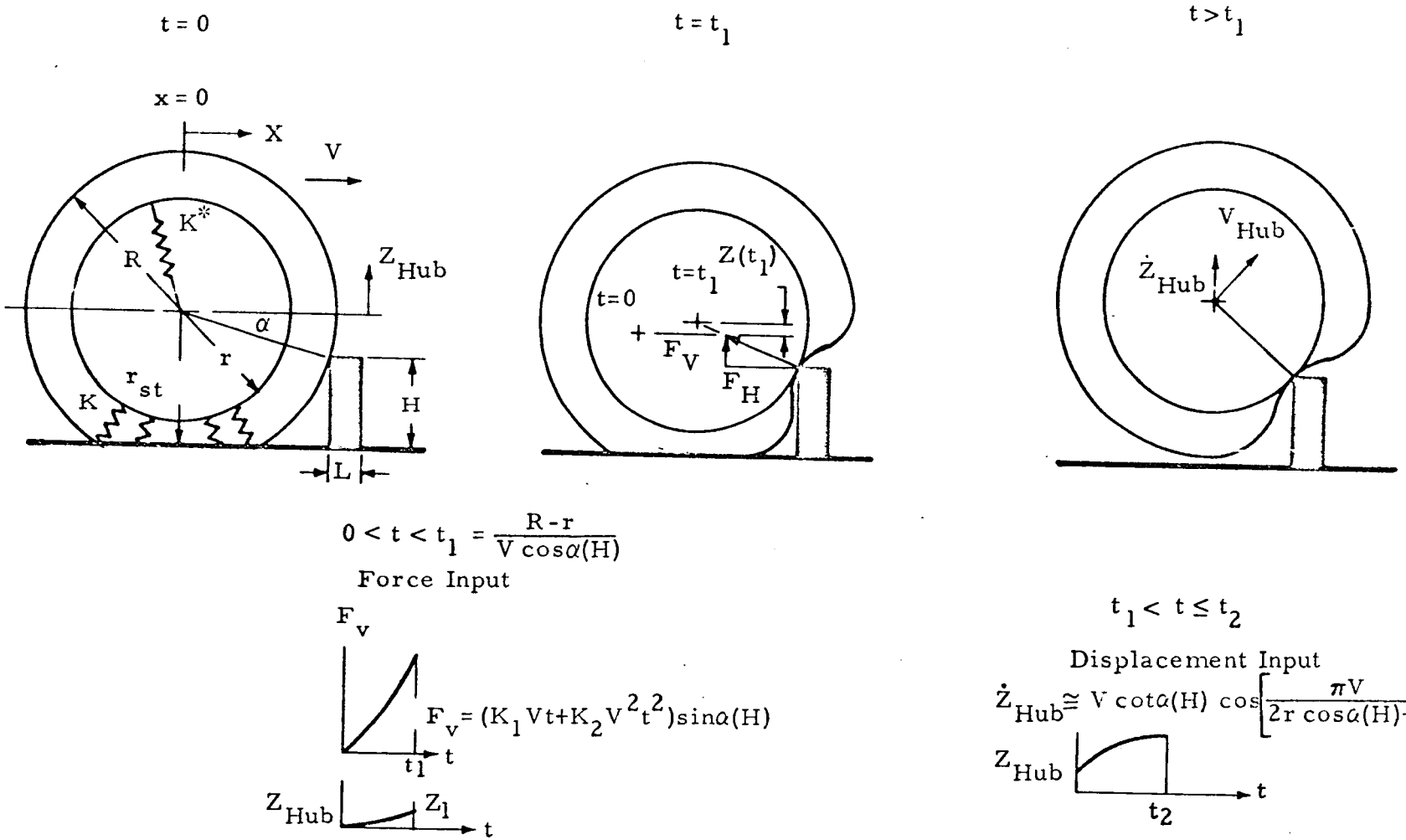

Figure 14 - Obstacle Simulation

Equation (3) is a realistic approximation until time t_2 when wheel hub is above the center of the obstacle. All peak values of forces, displacement rates and accelerations occur prior to t_2. Therefore, simulating Phase 1 and Phase 2 of hitting obstacles of realistic height H and length L at various speeds V is adequate for design and analysis of a vertical suspension system.

A similar approach is being developed for disturbances acting in the horizontal plane, which is necessary for the design and analysis of the trolley drive system.

LGS/LSV MATHEMATICAL MODEL

The analog computer mathematical model for the LGS/LSV System will be two-dimensional planar models for the roll and pitch directions. Typical model diagrams are shown in Figures 15 and 16. Note the provisions for a two-stage spring constant in each wheel and the viscous damped suspension system. The mathematical expressions take into consideration a free flight ballistic trajectory if the wheels leave the ground. Also, note the sign conventions for the dimensions Z, ϕ and θ. From Figure 15 the differential equation representing the vertical displacement time histories for each mass and the effects of roll and cable dynamics can be derived giving results as follows:

$$\ddot{Z}_1 = \frac{D_6}{M_1}(\dot{Z}_8 - \dot{Z}_1) + \frac{K_6}{M_1}(Z_8 - Z_1) - \left(\frac{K_1 + K_{11}}{M_1}\right)(Z_1 - Z_{01}) - g_L + \frac{F_{o_{18}}}{M_1} f_{18} \qquad (1)$$

where:

$(Z_8 - Z_1)$ limited $\pm S$

$-S_1 < (Z_1 - Z_{01}) < 0 \quad K_1 = \text{value} \quad K_{11} = 0$

$(Z_1 - Z_{01}) \leq -S_1 \quad K_1 = \text{value} \quad K_{11} = \text{value}$

$Z_1 > H_E = (H_A + \text{ground ref.}) \quad K = 0 \quad K_{11} = 0$

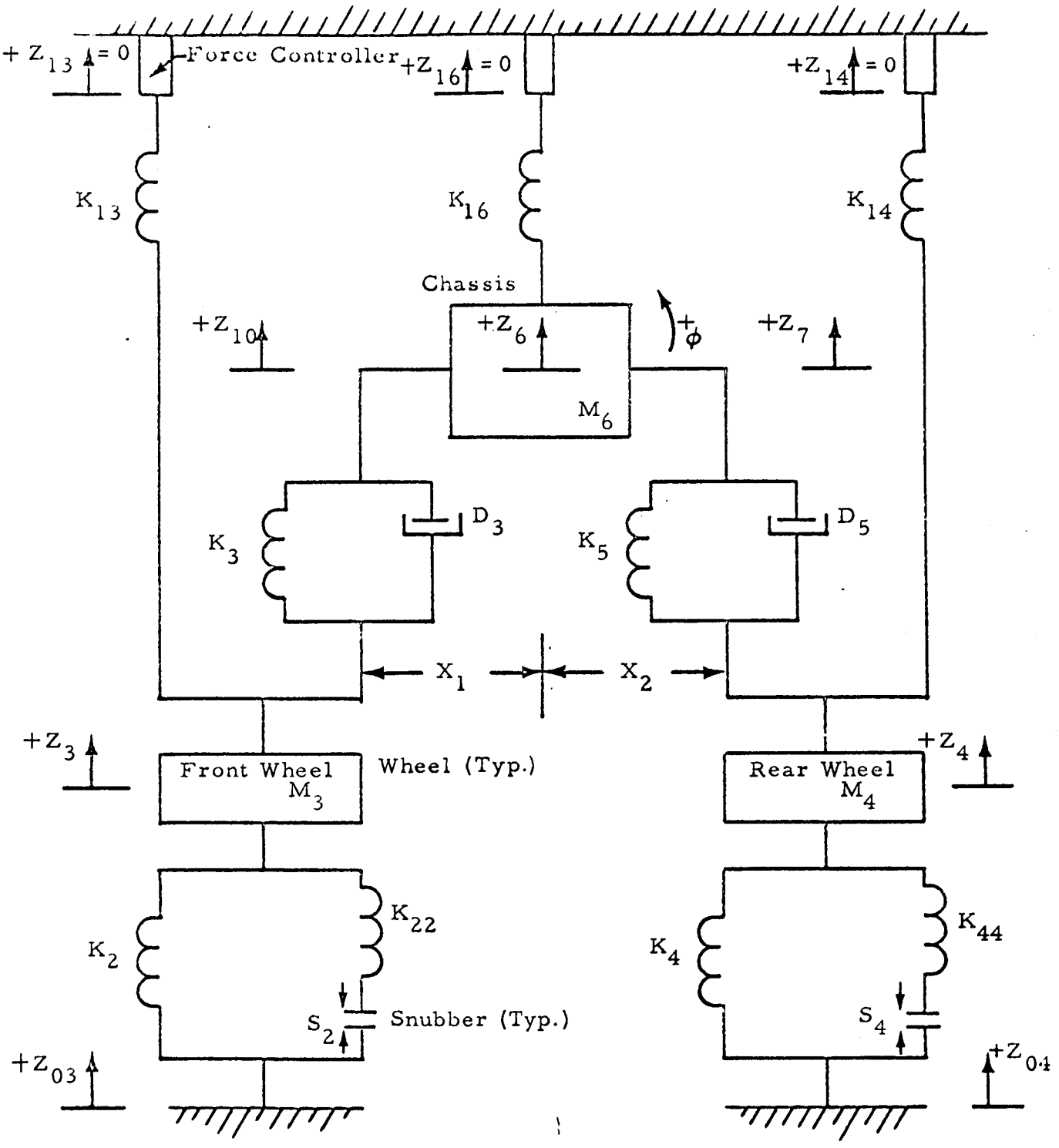

Figure 16 - Lunar Gravity Simulator Analog Simulator Diagram (Pitch Configuration)

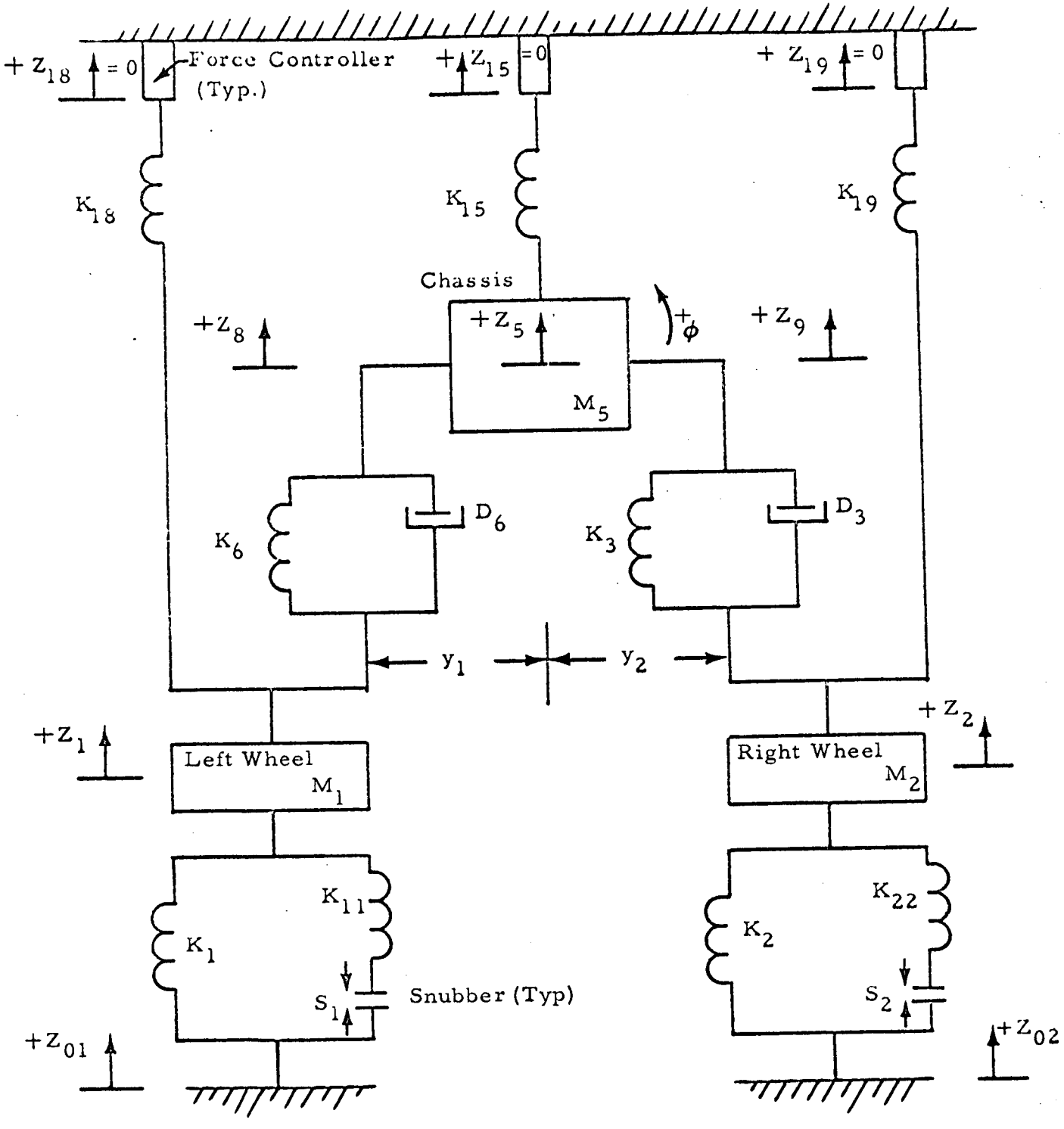

Figure 15 - Lunar Gravity Simulator Analog Simulation Diagram (Roll Configuration)

$$\ddot{Z}_2 = \frac{D_3}{M_2}(\dot{Z}_9 - \dot{Z}_2) + \frac{K_3}{M_2}(Z_9 - Z_2) - \frac{(K_2 + K_{22})}{M_2}(Z_2 - Z_{02}) - g_L + \frac{F_{o_{19}}}{M_2} f_{19} \quad (2)$$

where:

$(Z_9 - Z_2)$ limited $\pm S$

$-S_2 < (Z_2 - Z_{02}) < 0 \quad K_1 = \text{value} \quad K_{11} = 0$

$(Z_2 - Z_{02}) \leq -S_1 \quad K_1 = \text{value} \quad K_{11} = \text{value}$

$Z_2 > H_E = (H_A + \text{ground ref.}) \quad K_1 = 0 \quad K_{11} = 0$

$$\ddot{Z}_5 = \frac{D_6}{M_5}(\dot{Z}_8 - \dot{Z}_1) - \frac{K_6}{M_5}(Z_8 - Z_1) - \frac{D_3}{M_5}(\dot{Z}_9 - \dot{Z}_2) - \frac{K_3}{M_5}(Z_9 - Z_2) - g_L + \frac{F_{o_{15}}}{M_5} f_{15} \quad (3)$$

where:

$$\left.\begin{matrix}(Z_9 - Z_2) \\ (Z_8 - Z_1)\end{matrix}\right\} \quad \text{limited } \pm S$$

$$\ddot{\phi} = \frac{Y_1}{I_x}\left[K_6(Z_8 - Z_1) + D_6(\dot{Z}_8 - \dot{Z}_1)\right] - \frac{Y_2}{I_x}\left[K_3(Z_9 - Z_2) + D_3(\dot{Z}_9 - \dot{Z}_2)\right] \quad (4)$$

$$Z_8 = Z_5 - Y_1\phi \quad (5)$$

$$\dot{Z}_8 = \dot{Z}_5 - Y_1\dot{\phi} \quad (6)$$

$$Z_9 = Z_5 + Y_2\phi \quad (7)$$

$$\dot{Z}_9 = \dot{Z}_5 + Y_2\dot{\phi} \quad (8)$$

$$F_{o_{19}} = 5/6\, M_1\, g_E \quad (9)$$

$$F_{o_{19}} = 5/6\, M_2\, g_E \tag{9.1}$$

$$F_{o_{15}} = 5/6\, M_5\, g_E \tag{9.2}$$

$$K_{18} = \frac{E \cdot Ac_{18}}{Lc_{18}} \qquad \begin{array}{l} E = 17.3 \times 10^8 \text{ lb/pt}^2 \\ A = \text{area of cable} \\ L = \text{length of cable} \end{array} \tag{9.3}$$

$$K_{19} = \frac{E \cdot Ac_{19}}{Lc_{19}} \tag{9.4}$$

$$K_{15} = \frac{E \cdot Ac_{15}}{Lc_{15}}$$

$$f_{18} = -K_{18}\left[\frac{T_2 S+1}{E_1 S^2 + E_2 S+1}\right] \dot{Z}_1 \tag{10.1}$$

$$f_{19} = -K_{19}\left[\frac{T_2 S+1}{E_1 S^2 + E_2 S+1}\right] \dot{Z}_2 \tag{10.2}$$

$$f_{15} = -K_{15}\left[\frac{T_3 S+1}{E_3 S^2 + E_4 S+1}\right] \dot{Z}_5 \tag{10.3}$$

From Figure 16 the differential Equations representing the vertical displacement time histories for each mass and the effects of pitch and cable dynamics can be derived giving results as follows:

$$\ddot{Z}_3 = \frac{D_3}{M_3}(\dot{Z}_{10} - \dot{Z}_3) + \frac{K_3}{M_3}(Z_{10} - Z_3) - \frac{(K_2 + K_{22})}{M_3}(Z_3 - Z_{03}) - g_L + \frac{F_{o_{13}}}{M_3} f_{13} \tag{11}$$

where:

$(Z_{10} - Z_3)$ limited $\pm$ S

$-S_2 < (Z_3 - Z_{03}) < 0 \quad K_2 = \text{value} \quad K_{22} = 0$

$(Z_3 - Z_{03}) \leq -S_2 \quad K_2 = \text{value} \quad K_{22} = \text{value}$

$Z_3 \quad H_E = (H_A + \text{ground ref.}) \quad K_2 = 0 \quad K_{22} = 0$

$$\ddot{Z}_4 = \frac{D_5}{M_4}(\dot{Z}_7 - \dot{Z}_4) + \frac{K_5}{M_4}(Z_7 - Z_4) - \frac{(K_4 + K_{44})}{M_4}(Z_4 - Z_{04}) - g_L + \frac{F_{o_{14}}}{M_4} f_{14} \qquad (12)$$

where:

$(Z_7 - Z_4)$ limited $\pm$ S

$-S_4 < (Z_4 - Z_{04}) < 0 \quad K_4 = \text{value} \quad K_{44} = 0$

$(Z_4 - Z_{04}) \leq -S_4 \quad K_4 = \text{value} \quad K_{44} = \text{value}$

$Z_4 > H_E = (H_A + \text{ground ref.}) \quad K_4 = 0 \quad K_{44} = 0$

$$Z_6 = -\frac{D_5}{M_6}(\dot{Z}_7 - \dot{Z}_4) - \frac{K_5}{M_6}(Z_7 - Z_4) - \frac{D_3}{M_6}(\dot{Z}_{10} - \dot{Z}_3) - \frac{K_3}{M_6}(Z_{10} - Z_3) - g_L \qquad (13)$$

$$\frac{F_{o_{16}}}{M_6} f_{16}$$

where:

$$\left.\begin{matrix}(Z_7 - Z_4) \\ (Z_{10} - Z_3)\end{matrix}\right\} \quad \text{limited} \pm S$$

$$\ddot{\phi} = \frac{X_1}{I_Y}\left[D_3(\dot{Z}_{10} - \dot{Z}_3) + K_3(Z_{10} - Z_3)\right] - \frac{X_2}{I_Y}\left[D_5(\dot{Z}_7 - \dot{Z}_4) + K_5(Z_7 - Z_4)\right] \qquad (14)$$

$$Z_7 = Z_6 + X_2\theta \qquad (15)$$

$$\dot{Z}_7 = \dot{Z}_6 + X_2\dot{\theta} \qquad (16)$$

$$Z_{10} = Z_6 - X_1\theta \qquad (17)$$

$$\dot{Z}_{10} = \dot{Z}_6 - X_1\dot{\theta} \qquad (18)$$

$$F'_{o_{13}} = 5/6\ M_3\ g_E \tag{19}$$

$$F_{o_{14}} = 5/6\ M_4\ g_E \tag{19.1}$$

$$F_{o_{16}} = 5/6\ M_6\ g_E \tag{19.2}$$

$$K_{13} = \frac{E \cdot Ac_{13}}{Lc_{13}} \tag{19.3}$$

$$K_{14} = \frac{E \cdot Ac_{14}}{Lc_{14}} \tag{19.4}$$

$$K_{16} = \frac{E \cdot Ac_{16}}{Lc_{16}} \tag{19.5}$$

$$f_{13} = -K_{13}\left[\frac{T_2S+1}{E_1S^2+E_2S+1}\right]\dot{Z}_3 \tag{20.1}$$

$$f_{14} = -K_{14}\left[\frac{T_2S+1}{E_1S^2+E_2S+1}\right]\dot{Z}_4 \tag{20.2}$$

$$f_{16} = -K_{16}\left[\frac{T_3S+1}{E_3S^2+E_4S+1}\right] \tag{20.3}$$

The previous equations for the LGS/LSV mathematical model have been programmed on the Lockheed/HREC analog computers. Sample results are discussed in the following paragraphs of this report.

Continued study on this task will include incorporation of the LSV wheel input equations derived in this report into the overall LGS/LSV mathematical model. Also, mathematical expressions for the trolley drive system will be derived and incorporated into the analog simulation.

LGS SAMPLE ANALOG OUTPUT DATA

Sample analog results are shown in Figures 17 and 18. The sample case was chosen to show the expected worst results for an input of +1.0′ step for two seconds, then a -1.0′ hole for three seconds, and then a +1.0′ step to return to ground level.

Table 2 gives the maximum and minimum value for the roll configuration. To show the typical roll angle, both left wheels were disturbed simultaneously by the input described above. Note that for the 1.0 ft step height, the body mass rotated -60.7°. For a 0.5′ step the body mass rotated only -30° which suggests that a step height of +1.5′ would cause the vehicle to overturn.

Table 3 gives the maximum and minimum value for the pitch configuration. To show a severe case, the front wheel was disturbed by the above described input then two seconds later the rear wheel was allowed to hit the same disturbance. This corresponds to a vehicle velocity of approximately 7.3 km/hr. This timing allowed the front wheel to be in the hole at the same time the rear wheel hit the initial step. Pitch rates of 100°/sec and pitch angles of 53° were observed.

The wheel was simulated to represent the actual wheel effect as closely as possible. The simulation was accomplished by allowing the outer wheel to compress to the rigid inner wheel (snubbing) and if necessary, the wheel can also leave the ground (ballistic flight). Note that Z_3 (Figure 18) reached +7.5 feet which is 6.5 feet greater than the step input. This ballooning effect would cause some major problems in lunar travel.

The delta forces in each cable (f) represented by $f_{13}, f_{14}, f_{15}, f_{16}, f_{18}, f_{19}$ are normalized to be zero under static condition and represent the dynamic variation from the static forces ($F_{o_{13}}$ for f_{13} as an example) before the wheel inputs are applied. From Table 3 the maximum ΔF is 1% of the static cable force. The transfer functions representing the cable dynamics are

Table 2

ROLL DATA - REFERENCE FIGURE 17

VARIABLE	UNITS	MAX	MIN
$\dot{Z}_1$	ft/sec	+34.0	-9.5
$\dot{Z}_1$	ft	+6.8	-1.6
Obst(Z_1)	ft	+1.0	-1.0
$\dot{Z}_2$	ft/sec	+1.5	-3.5
Z_2	ft	-0.12	-0.17
Obst(Z_2)	ft	0	0
$\dot{Z}_5$	ft/sec	+4.0	-4.7
Z_5	ft	+3.0	-1.7
ϕ	rad/sec	+1.4(80°/sec)	-1.35(77.3°/sec)
ϕ	rad	0.33(19°)	-1.06(60.7°)
f_{18}	%	+2.0	-9.0
f_{19}	%	0	0
f_{15}	%	+0.8	-2.8

Table 3

PITCH DATA - REFERENCE FIGURE 18

VARIABLE	UNITS	MAX	MIN
$\dot{Z}_3$ Front Wheel	ft/sec	+36.0	-10.0
Z_3 Front Wheel	ft	+7.5	-1.6
Obst(Z_3)	ft	+1.0	-1.0
$\dot{Z}_4$ Rear Wheel	ft/sec	+36.0	-13.0
Z_4 Rear Wheel	ft	+9.3	-1.6
Obst(Z_4)	ft	+1.0(1 sec delay)	-1.0(1 sec delay)
$\dot{Z}_6$ Chassis	ft/sec	+6.5	-5.5
Z_6 Chassis	ft	+3.7	-2.5
$\dot{\theta}$	rad/sec	+1.75(100°/sec)	-1.3(74.4°/sec)
θ	rad	+.92(52.8°)	-.66(37.9°)
f_{13}	%	+2.3%	-9.3%
f_{14}	%	+2.5%	-10.0%
f_{16}	%	+1.0%	-3.0%

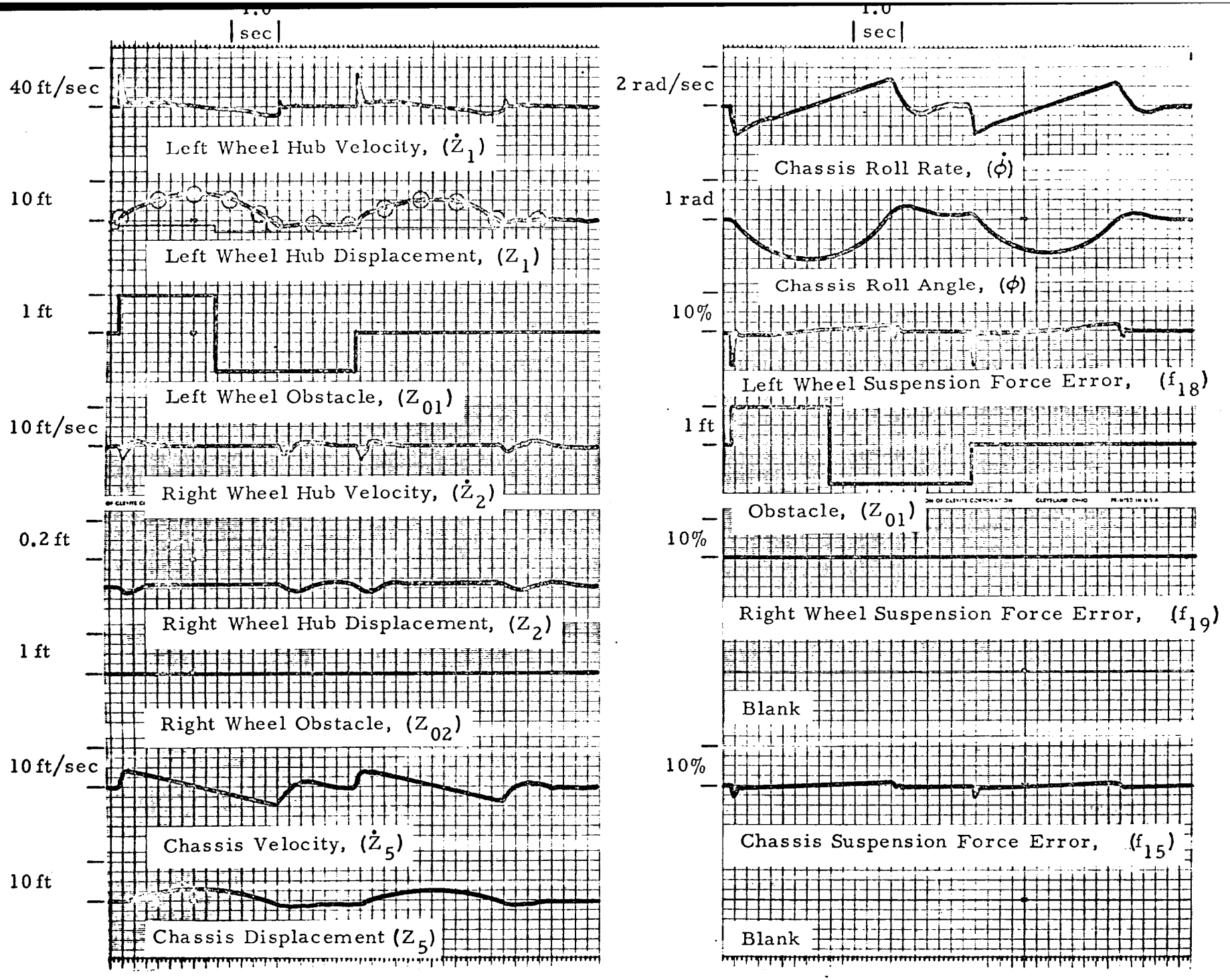

Figure 17 - Lunar Gravity Simulation Bendix LSSM Analog Results, Roll Configuration

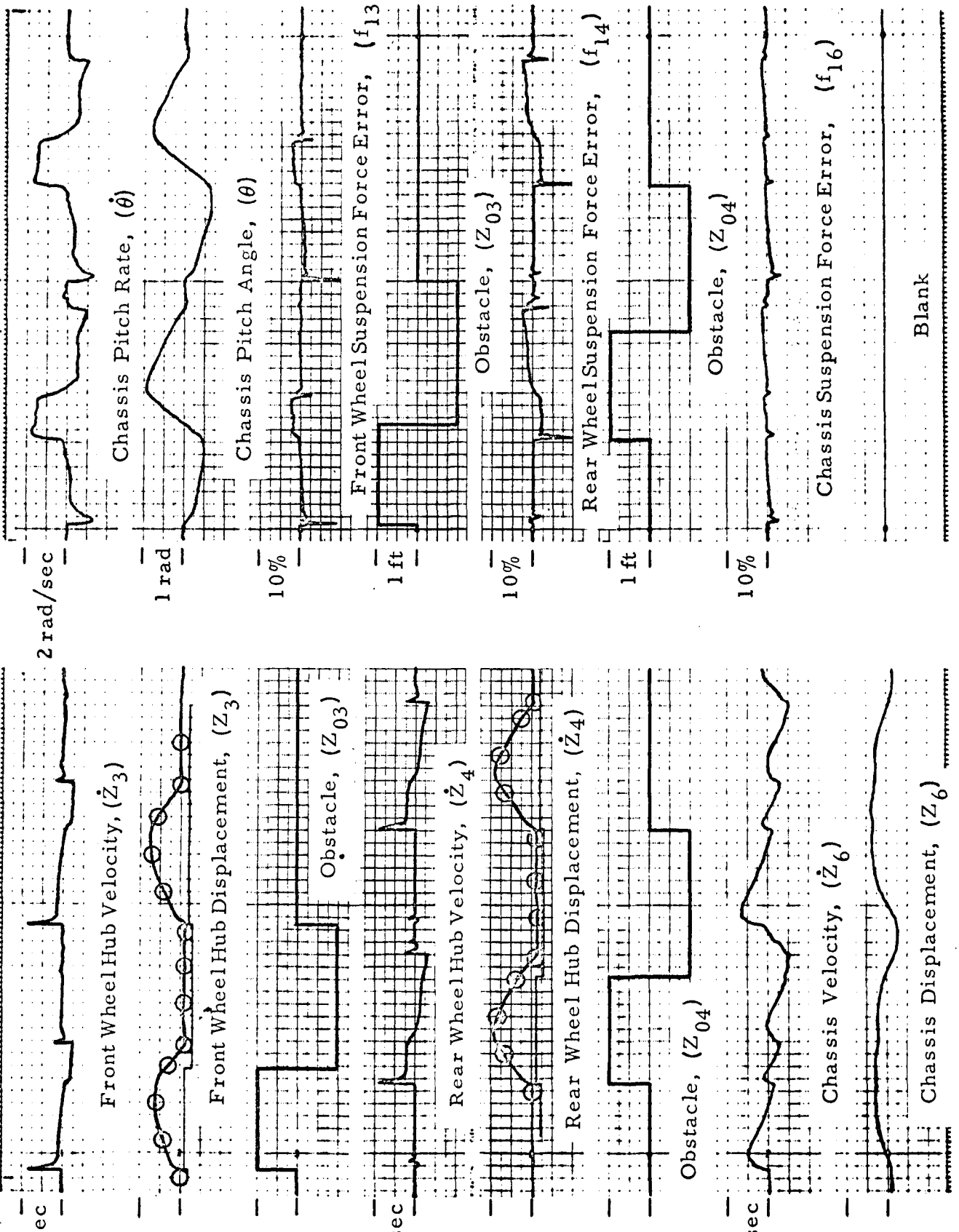

Figure 18 - Lunar Gravity Simulation Bendix LSSM Analog Results, Pitch Configuration

second-order and do not at present include the cable and winch inertias. The error is expected to increase with the addition of these inertias.

The acceleration outputs were not recorded due to the use of step inputs which give very high acceleration and cannot be recorded accurately. The hub force input described earlier will be applied next and will give realistic acceleration times.

Section 5
TWO-DIMENSIONAL LGS SYSTEM DESIGN

Initial efforts on the two-dimensional LGS system design were directed toward establishing the suspension platform size, determining LGS/LSV attachment interface, and establishing an overall LGS baseline concept. These three basic areas are discussed in the following paragraphs.

SUSPENSION PLATFORM SIZE

Determination of the suspension platform size was accomplished by a composite layout of LSV configurations under study. These LSV's include both the LSSM and MOLAB concepts of Boeing and Bendix as shown in Figure 19. The platform size sufficient to provide suspension attachment points for the wheels and chassis arrangements is approximately 160 inches (4.06 m) x 255 inches (6.48 m). This allows sufficient spacing for cable vertical alignment compensation for vehicle roll and pitch angles up to approximately 35°. The composite layout in Figure 19 assumes a common c.g. location relative to the suspension platform for all LSV's except for those involving a trailer. In this case, the trailer pivot point is determined by the heaviest vehicle and the trailer/platform pivot points for lighter trailer configuration LSV's are aligned rather than the c.g. locations.

The following criteria will be used for the structural design of the suspension platform.

1. Maximum LSV weight will be 10,000 lb (4500 kg). The trailer and wheel weights will be proportioned according to the Bendix and Boeing MOLAB concepts.
2. Trailer pivot structure will be sized according to the maximum trailer gross weight (chassis plus wheels).

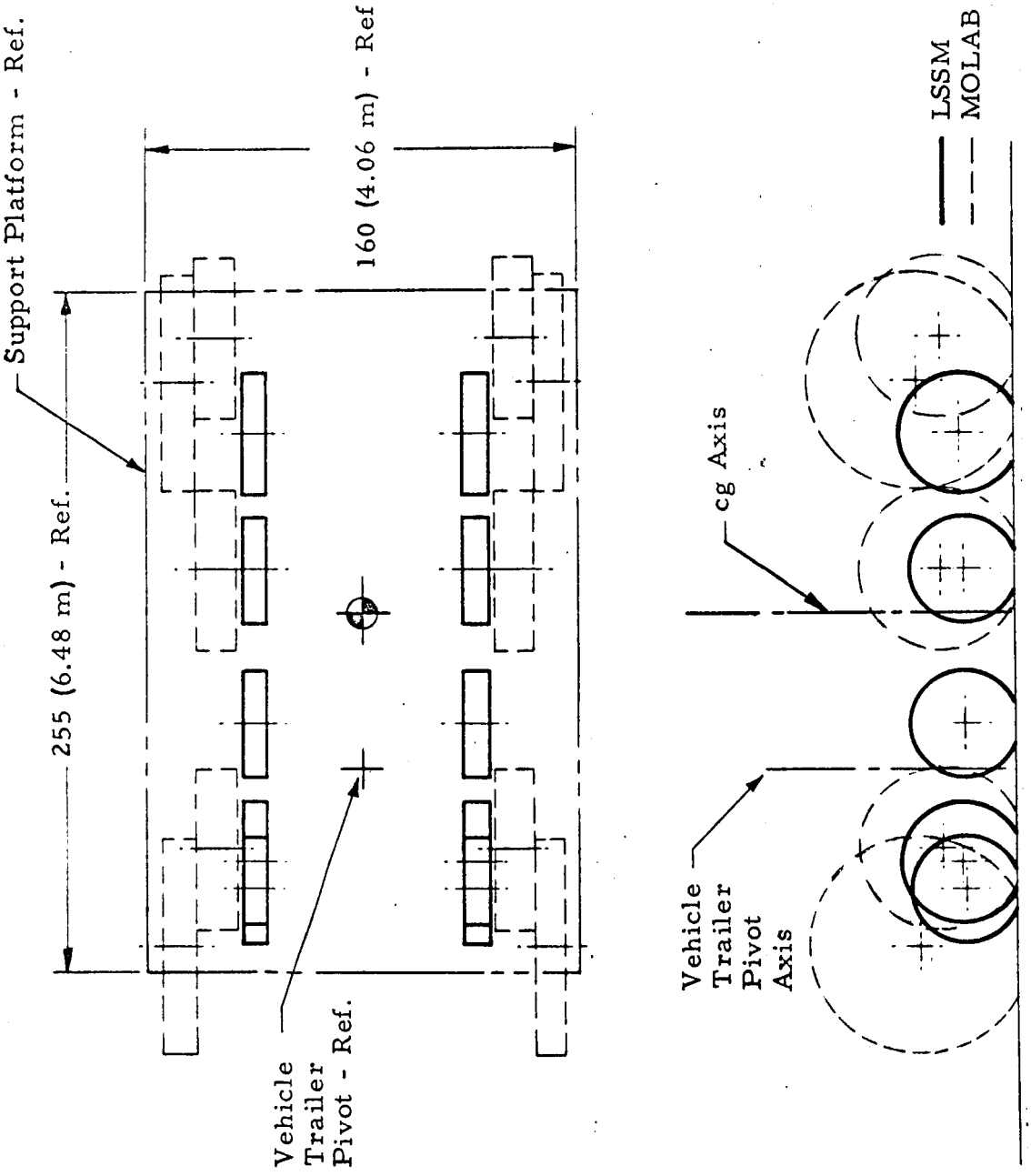

Figure 19 - Composite Lunar Surface Vehicle Layout

3. Structural natural frequency of the platform will be approximately 5 times the applied frequencies from the suspension cables. The design natural frequency is anticipated to be on the order of 10 - 12 cps.
4. Attachment points for the LSV chassis will provide for any one of the following:
   a. At the chassis c.g.
   b. At two points on the LSV roll axis (thru the c.g.).
   c. At two points on the LSV pitch axis (thru the c.g.).

The trailer chassis attachment will be at its c.g.

LGS/LSV ATTACHMENT INTERFACE

It is believed that the attachment points at the LSV chassis can be accomplished by a simple tubular truss frame between the chassis frame and a universal joint on the vehicle roll or pitch axis. No particular problem is anticipated in accomplishing this and maintaining an accurate 1/6 g simulation. However, attachment to the LSV wheels may present somewhat more of a problem. Figure 20 depicts an LSV suspension system attachment arrangement which has considerable merit and is recommended for further study. This arrangement consists of a special shaped light weight support frame which is attached so that the wheel has adequate roll and pitch freedom, and the suspension cable tension vector is aligned as closely as possible to the LSV suspension system center of gravity. A universal joint couples the LGS support frame to the LSV suspension. Further analysis on this arrangement will consist of studying the effects of attachment point c.g. offset and LGS attachment frame mass on lunar g error. The results of this analysis should define the wheel attachment point design criteria.

LGS SYSTEM CONFIGURATION

Figure 21 depicts a two dimensional LGS configuration which can be expanded to a three-dimensional system. The common system elements between the two configurations is the suspension platform with the associated suspension devices and the 2-D "X" drive system. The suspension

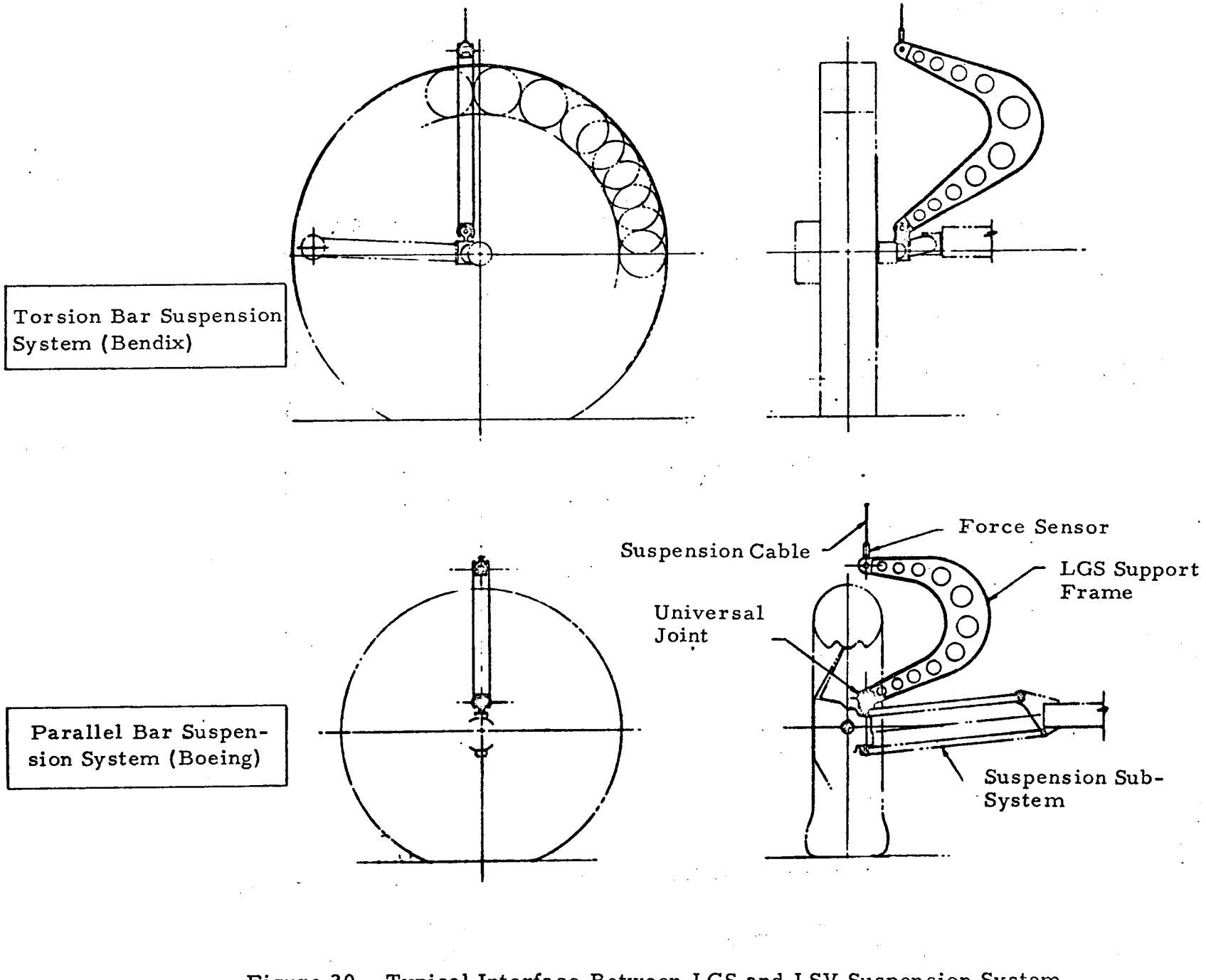

Figure 20 - Typical Interface Between LGS and LSV Suspension System

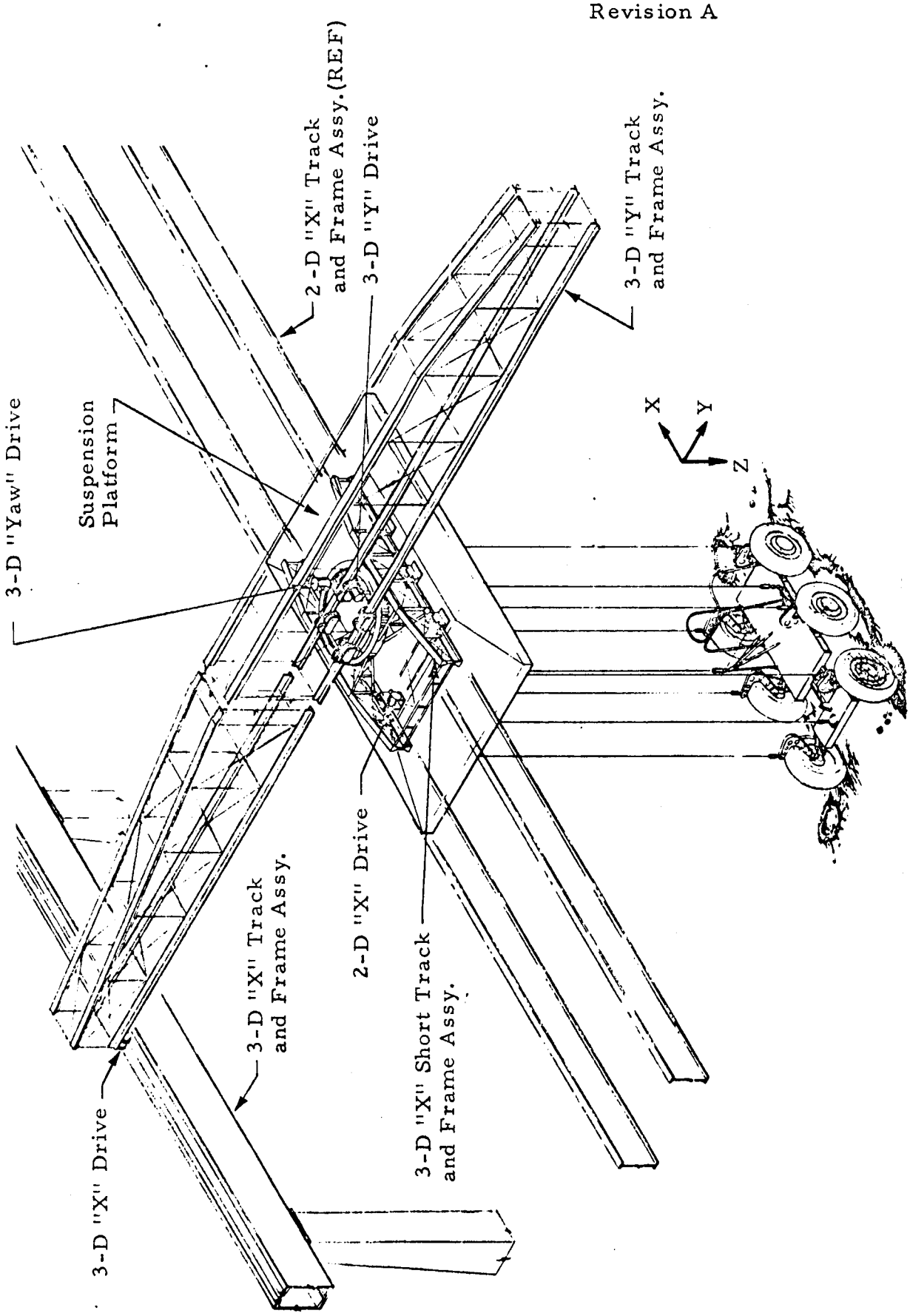

Figure 21 - Lunar Gravity Simulator System Configuration

platform would be a light weight structure designed to support the anticipated range of LSV's and to accept the high transient accelerations necessary to minimize the fore and aft acceleration error by maintaining an exacting horizontal relative positioning between suspension platform and the LSV. This is essential in maintaining the suspension cable vertical alignment. The 2-D "X" drive system would be designed accordingly. This drive system and the associated track guide rollers would be interchangeable between the 2-D "X" Track and Frame Assembly and the 3-D "X" Short Track and Frame Assembly. The latter would facilitate high transient accelerations over a short stroke when the system is expanded to a 3-D configuration.

Expansion of the 2-D LGS system to a 3-D system would involve the addition of the following major elements.

1. 3-D "X" short track and frame assembly with the associated yaw bearing assembly.
2. 3-D "yaw" drive system and the associated controls.
3. 3-D "Y" drive system and the associated controls. The "yaw" and "Y" sensor and control system would be an integrated system probably using a common displacement sensor.
4. 3-D "Y" track and frame assembly.
5. 3-D "X" drive system - this system would sense the displacement of the short stroke "X" system and control accordingly to null the middle of the short stroke.
6. 3-D "X" track and frame assembly and the associated support structure.

Section 6
CONCLUSIONS AND RECOMMENDATIONS

The results of the tasks performed during the first five week study effort suggest the following conclusions and recommendations.

1. A literature survey indicates that the information available on the design of gravity simulators is limited to three basic areas: (1) the MSFC studies by Northrop Space Laobratories; (2) the MSC Space Motion Simulator Studies by Aircraft Armaments, Inc.; and (3) the facilities for gravity simulation built by the Langley Research Center. These are listed in the order of their relative importance to the LGS studies in process by Lockheed.

2. The suspension device concept should consist of independent cables for each mass to be suspended. This is recommended, instead of the intermediate wheel suspension harness arrangements which present dynamic problems in the suspension cables.

3. A suspension device force control system consisting of a servo controlled hydraulic motor driven cable is the system recommended for further study. This appears to be a very workable solution and possibly the best approach to the problem of force control with large displacements.

4. Displacement error sensors for the trolley positioning system should use a photovoltaic sensor concept for best accuracy. Alternatively, an angle sensing potentiometer which senses the suspension cable angle deviations is recommended for comparison. The latter is believed to be considerably less accurate but is simpler and less expensive.

5. The LGS/LSV mathematical model, step function obstacles and wheel dynamic simulation described in Section 4.0 of this report are recommended for evaluating the LGS performance parameters. The mathematical model described will be further refined to include the trolley drive system dynamics.

6. The LSV suspension system attachment methods (Figure 20) and the overall LSG Configuration (Figure 21) described in Section 5.0 of this report are recommended for further study.

Section 7
FUTURE WORK

Continued study effort for the next five-week period is recommended in the following areas which are outlined in accordance with the Program Plan tasks of Figure 1.

Task	Continued Study Efforts
1.2	Refine mathematical model of the 2-D LGS/LSV system to include the trolley drive system dynamic simulation and the wheel dynamic input simulation described in Section 4 of this report.
1.3	Continue the analysis and selection of suspension device and drive system concepts. These study efforts will be continued along the lines described in Section 3 of this this report.
1.4	Conduct a dynamic analysis of the 2-D LGS and determine the LGS/LSV interaction and Lunar "g" error.
1.5	Conduct an analysis of the LGS system to determine the pertinent tradeoffs between rail height and LGS system parameters.
1.6	Conduct a cost analysis of the 2-D Lunar Gravity Simulator. This analysis will include only the essential elements of the system which are a part of the preliminary design and analysis study.
1.7	Continue the design, layout and component, specification analysis for the 2-D LGS system.

These tasks are scheduled to be completed during the next five-week study period.